1998 April 20
Report No. C97-38411-R3

DOE/ID/13238--T1

ALCOA TECHNICAL CENTER

100 TECHNICAL DRIVE • ALCOA CENTER, PA 15069-0001

Spray Forming - Aluminum

Third Annual Report (Phase II)

Technical Progress - Summary

Submitted to:
U. S. Department of Energy

Submitted by:
Aluminum Company of America
Alcoa Technical Center
100 Technical Drive
Alcoa Center, PA 15069-0001

ALCOA

Creating Value through Technology

DOE/ID/13238--T1

Spray Forming - Aluminum

Third Annual Report
(Phase II)

Technical Progress - Summary

1998 April

Work Performed Under Contract:
DE-FC07-94ID13238

Reported by:
Robert L. Kozarek
Principal Investigator

Prepared for
U.S. Department of Energy
Field Office, Idaho Falls, ID
Sponsored by the Office of the Assistant Secretary for
Energy Efficiency and Renewable Energy
Office of Industrial Technologies
Washington, D.C.

Prepared by
Aluminum Company of America
Alcoa Technical Center
100 Technical Drive
Alcoa Center, PA 15069-0001

DISCLAIMER

DISCLAIMER

Portions of this document may be illegible electronic image products. Images are produced from the best available original document.

ABSTRACT

Commercial production of aluminum sheet and plate by spray atomization and deposition is a potentially attractive manufacturing alternative to conventional ingot metallurgy/hot-milling and to continuous casting processes because of reduced energy requirements and reduced cost. To realize the full potential of the technology, the Aluminum Company of America (Alcoa), under contract by the U.S. Department of Energy, is investigating currently available state-of-the-art atomization devices to develop nozzle design concepts whose spray characteristics are tailored for continuous sheet production. This third technical progress report will summarize research and development work conducted during the period 1997 October through 1998 March. Included are the latest optimization work on the Alcoa III nozzle, results of spray forming runs with 6111 aluminum alloy and preliminary rolling trials of 6111 deposits.

TABLE OF CONTENTS

LIST OF TABLES

LIST OF FIGURES

LIST OF FIGURES (CONT'D)

0.0 INTRODUCTION/BACKGROUND

In April of 1994, the Department of Energy's Office of Industrial Technology entered into a Cooperative Agreement with the Aluminum Company of America (Alcoa) on the project titled: Spray Forming of Aluminum. Spray forming technology is based on the atomization of liquid melts and subsequent deposition on a substrate (see Figure 0.1). The objectives of this process development project are to show the technical and economic viability of an aluminum spray forming process for sheet products and to develop an investment strategy for technology transfer.

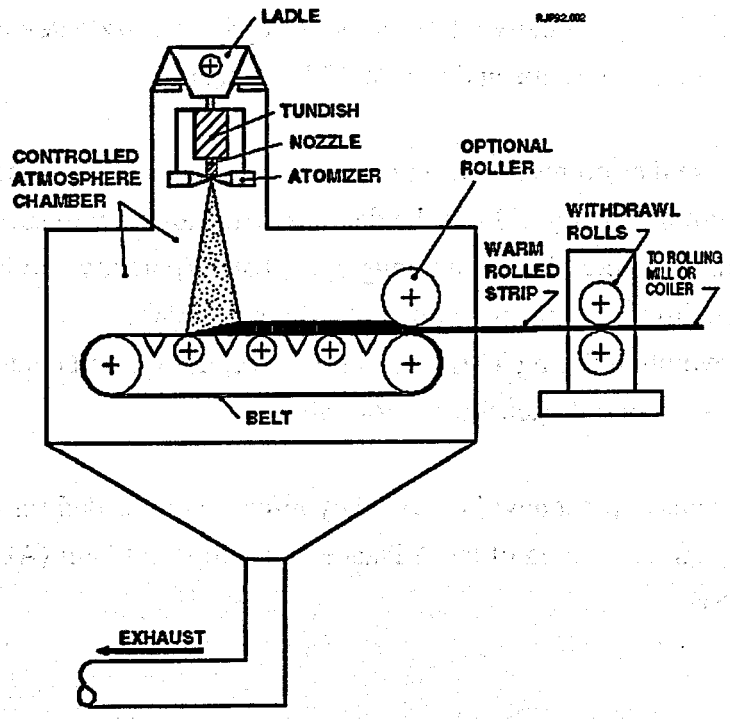

Figure 0.1: Production of Sheet Materials via Spray Forming - Concept Drawing

The Alcoa work has focused on translating bench-scale spray forming technology into a near-commercial, cost effective aluminum sheet production process as a manufacturing alternative to conventional ingot casting-hot rolling processes. Major subcontractors throughout the program have included Air Products & Chemicals, Inc. (APCI), Idaho National Engineering and Environmental Laboratory (INEEL), Massachusetts Institute of Technology

(MIT), Carnegie Mellon University (CMU), Drexel University, and the University of California-Irvine (UCI).

The Alcoa contract, which expired in April of 1997, was re-activated in October of 1997 after acceptance of a new Technical and Cost Proposal to complete the last three years of the program. With the overall reduction in program scope, Alcoa has modified its technical approach to address key technical/commercialization issues prior to committing to the construction of an Advanced Development Unit (ADU). The approach includes:

1. Using the existing Tafa bench scale unit to extend as much as possible spray forming process knowledge specifically related to issues of spray nozzle development, control of porosity, and control of shape and profile of the deposit.

2. Developing base thermo-mechanical processing (TMP) technology using commercially significant aluminum alloy 6111 as the demonstration alloy, with special focus given to:
   - As cast microstructural quality throughout a batch (porosity and inclusions).
   - Surface quality development with and without scalping.
   - Porosity evolution during TMP--Final pore morphology and content.
   - Mechanical properties (tensile and formability).

It is expected that this approach will provide key information needed for the design, construction and commissioning of the Advanced Development Unit (ADU), and for the investment analysis.

1.0 IMPROVE PROCESS UNDERSTANDING AND CAPABILITY

The objective of Task 1 is to increase our understanding of the spray forming process parameters at bench-scale. Included are nozzle optimization, mathematical modeling and performance of parametric studies, specification of baseline thermo-mechanical processing (TMP) parameters, and definition of the potential larger scale process operating conditions. Work for this period included nozzle optimization and characterization in water spray studies; process development studies in the Tafa unit for producing deposits for rolling studies; parametric studies in the Marko unit for porosity formation; equipment modifications for improved operational efficiency; deposit characterization and preliminary rolling (TMP) studies; and model development for chamber design and porosity studies.

1.1 Nozzle Development - Water Spray Studies

Nozzle development for this reporting period has focused on optimizing the setup and operation of the 8-inch Alcoa III linear nozzle system for producing a flat deposit profile.

The Alcoa III linear nozzle system is shown in Figure 1.1.1. Figure 1.1.2 shows a transverse cutaway. A metal gauze type packing material is used inside to distribute flow from the inlet pipes to the gas slits. Note the gas slit opening and the metal delivery tip protrusion distance can be changed. A key feature of the nozzle is the ability to adjust individual pressures to control the shape of a sprayed deposit. Under normal operating conditions, the nozzle is operated in a symmetric fashion in which pressure settings on the upstream and downstream halves of the nozzle are from a common source, and chamber pressures P1 and P2 are set equal to P5 and P4 respectively (see Figure 1.1.2).

The converging/diverging geometry of the exit gas slit results in an overexpanded supersonic gas jet at pressures greater than the critical pressure (approximately 23 psig). The nozzle was designed to operate in a relatively low pressure range of 40-80 psi to minimize compressor costs. For spray forming, the nozzle is operated by adjusting the gas to metal ratio (G/M) to control the fraction solid in the spray. The pressures P1→ P5, are adjusted relative to each other to control the shape of the deposit. The protrusion distance and gap are set according to the desired atomizing behavior. Water spray tests are used extensively to establish the operating characteristics of the nozzle such as gas and liquid flow rates as functions of pressure, aspiration pressure, geometrical effects such as protrusion length on spray profile.

Water spray tests are performed on a separate test stand using a spray patternator (Figure 1.1.3). Nitrogen atomizing gas for the test stand is now supplied from the Tafa unit. This substantially increases the gas supply rate for water testing and provides identical instrumentation and control.

1.1.1 Flow Rate Control

The gas flow rate is adjusted to achieve the desired gas to metal ratio (G/M).

The liquid delivery tip of the nozzle uses a series of holes aligned along the length of the tip and sized to give the desired flow rate at typical metal head pressure. The confined gas jet surrounding the liquid delivery tip also affects the metal delivery rate due to aspiration. The aspiration pressure is added to the head pressure to determine the metal flow rate. Aspiration effects can be positive or negative increasing or choking liquid flow, respectively. As reported by N. Grant in Phase I of the Spray Forming Project [2], one of the biggest factors affecting the aspiration pressure at the nozzle tip is the protrusion length of the liquid delivery tip.

Aspiration pressure has been determined empirically by two means. The first is a static measurement of the pressure (or vacuum) inside the liquid delivery tip with gas flow only such as performed by Grant, et al. [2] The second is a dynamic measurement of the change in head pressure with and without gas flow at a constant liquid flow rate. Aspiration pressures measured by the first method are generally greater than the latter, however, the latter method is believed to provide a better number for computing liquid flow rate changes resulting from aspiration effects because it more closely represents atomizing conditions.

1.1.2 Mass Flux Profiles

The deposit shape is directly controlled by the mass flux profile of the nozzle. Following the approaches reported earlier [1,3] water spray patternation was used extensively to determine the factors controlling the mass flux profiles of the spray.

Short axis spray profile

The short axis spray profile does not directly affect the shape of the deposit, but it is important to measure and understand effects on the process such as leading edge and trailing edge

effects as well as process effects which are deposition rate sensitive such as mushy layer thickness.

Patternator studies show the short axis profile to be typically Gaussian shaped (Figure 1.1.4). The spray angle (spray width) and peak height vary according to the protrusion length. There is a rough trend towards a narrower spray as the protrusion length increases.

Long Axis Spray Profile

The long axis spray profile is directly related to the strip profile. The enabling technology of the Alcoa III nozzle is the ability to control the shape of the long axis mass flux profile. The basis for the pending patent is to break up the nozzle gas plenum into zones along the linear section and locally adjust the outlet gas dynamics to compensate for the natural tendency of the spray to assume a Gaussian distribution downstream. This is typically accomplished by varying the pressure in each zone. Using water spray testing, a large number of iterations can be tested off-line in a relatively short time. We have established a set of heuristic rules for adjusting pressures. These are illustrated on Figures 1.1.5-1.1.10.

Pressure Adjustments

With the Alcoa III nozzle, profile shape control is accomplished by adjusting the individual chamber pressures P1-P5. In the ensuing discussion, side to side symmetry is assumed, i.e. P1 = P5, P2 = P4. Figure 1.1.5 shows the typical Gaussian profile obtained when all the chamber pressures are set the same. Figure 1.1.6 shows the profile when the end chamber pressures, P1 & P5 are lowered. This widens the spray and also creates an unexpected double humped profile. Decreasing the center pressure slightly (holding the others constant) will flatten the spray profile as shown in Figure 1.1.7.

Figures 1.1.8-1.1.10 show the idealized response of the nominally flat profile, as represented by Figure 1.1.7, to increasing and decreasing one set of zone pressures while holding the others constant. In each of the figures, the area under the curves represents a constant spray volume. An analogy to interpreting shape changes is to imagine a water filled bladder resting on a flat surface. The overall top profile will be flat. If the bladder is impinged by a jet of gas, the gas will displace fluid to other regions. By extending this analogy to a series of jets it is possible to visualize the effects of pressure adjustments.

Figure 1.1.8 shows the result of changing the end chamber pressures, P1 and P5. When the end pressure is decreased the spray profile becomes wider and less defined as illustrated by the first band. When the end chamber pressure is increased the spray narrows and the profile becomes more concentrated in the center and is more humped.

Figure 1.1.9 shows the result of changing the transition chambers, P2 and P4. When the pressure is increased, it has an effect similar to decreasing the end pressure but the profile becomes wider or more spread out. When the pressure is decreased, the profile will take on a double humped shape which is more concentrated in the center than the next case.

Figure 1.1.10 shows the result of changing the center pressure, P3. The response at first glance seems similar to the transition chambers, however there are subtle differences. When the center pressure is decreased, the overall width of the profile does not change drastically, but the profile will have a strong central hump. The central hump becomes inverted creating a double humped profile when the center pressure is increased. The double humped profile remains wider than when the transition pressures are decreased.

Following the analogy presented above, pressure adjustments for spray trials and metal spray tests can be made to produce flat profiles.

1.1.3 Other Factors

Other factors which have been observed to affect the profile adjustments are various combinations of baffles and the type of packing materials in the zones. For example, at low operating pressures there are observable voids in the spray pattern at the location of the baffles. Therefore, we find it necessary to operate without baffles. As the nozzle pressure is increased the range of pressure adjustment is not enough to flatten the spray profile. So it is necessary to use the end baffles. As the pressure is increased further, it is necessary to use all of the baffles and to create separate zones for each gas feed.

A simplified explanation for this behavior can be made on the basis of cross talk between zones. That is, gas from one inlet operating at a higher pressure than adjacent inlets is transported through the packing material and baffles to adjacent zones. In the absence of baffles the pressure increases in all the zones due to cross talk. When baffles are installed they significantly decrease the cross talk. Changing the packing material alters the response.

In all cases, however, there is still enough cross talk that one cannot reliably predict the output pressure response to a set point change, it must be measured.

To improve the predictability of the response to a set point change, several improvements will be implemented. 1) Develop a uniform density packing material to diffuse the inlet gas jet and create a repeatable flow resistance between chambers. 2) Develop an internal flow model of the nozzle so that output pressures can be predicted on the basis of set point pressure settings.

1.2 Process Development - Metal Spray Tests

Metal spray tests were conducted in both the Tafa and Marko units with 6111 aluminum alloy. The Marko spray tests were run to determine spray settings for the Tafa unit. Spray tests in the Tafa unit were primarily conducted to produce deposits for rolling trials. Run parameters were selected to produce flat profiles and a range of deposition conditions affecting porosity, deposit width, thickness, and microstructure. Presently, a model-assisted designed experiment is being conducted to study the effects of processing conditions on porosity development in 6111 deposits.

1.2.1 TAFA Metal Spray Studies

During this period, a total of 14 runs were made in the Tafa unit using the Alcoa III nozzle system. All runs were made using 6111 alloy with the modified metal delivery tip described in the Second Annual Report [1] in which the slit opening was replaced by a series of holes. Since the primary purpose of the runs was to produce deposits for rolling investigations, deposition conditions were systematically adjusted with the aim of first producing the desired microstructure and then to optimizing the profile for flatness. Process parameters varied were the spray distance, gas flow rate (gas/metal ratio), nozzle protrusion length, substrate material, substrate width, substrate speed, and nozzle chamber pressures. In addition, argon and vacuum degassing steps were added to remove hydrogen from the molten aluminum charge. Table 1.2.1 summarizes the run parameter matrix. Of the 14 runs, 5 deposits were selected for preliminary rolling trials. Each deposit is representative of the extremes in the range and types of porosity. Observations on the effects of process parameters on the deposit are briefly discussed below.

6111 alloy

Automotive alloy 6111 sprays much like 6061 did in previous tests. In general, under the same spray conditions as alloy 3003, 6111 spray deposits appear to be more "dry" and prone to feathering around the edges of the deposit (See Figure 1.2.1). According to Osprey Metals, Ltd. [5] feathering is characteristic of 6XXX alloys.

Table 1.2.1: Tafa Run Parameter Matrix

Run No.	Spray Distance (inches)			Gas Flow Rate (lb/min)			Nozzle Protrusion Length (inches)			Substrate Width (in)		Substrate Speed (in/min)	
	Multi-level	19.5"	15.5"	< 40	~ 45	~ 60	0.12	0.115	0.18	5	8	< 100	> 110
104	X			X			X				IB	X	
105	X					X			X		IB	X	
106	X				X				X		SS		X
107	X				X				X	SS			X
108		X			X				X	SS			X
109		X			X				X	SS			X
110			X		X				X	SS			X
111			X		X				X	SS			X
112		X			X				X	SS			X
113		X			X			X		SS			X
114		X			X			X		SS		X	
115		X			X			X		SS		X	
116		X				X		X			SS	X	
117		X				X		X			SS	X	

IB = Foil Coated Insulating Board
SS = 1/2" Stainless Steel

Substrate Material

The properties of the substrate material are known to affect the thickness of the porous layer next to the substrate. Prior studies [3] showed that restricting substrate-side heat transfer will minimize bottom porosity and maximize useable deposit. An insulating board substrate with an aluminum foil cover was tried. It is necessary to cover the board materials to prevent

outgassing of adsorbed water which results in large bubbles under the deposit. The foil/insulator combination eliminated bottom porosity, however, the foil wrinkled to such an extent that there was not enough usable deposit for rolling trials. This approach has been abandoned temporarily in favor of a solid stainless steel substrate. With the stainless substrate the bottom surface of the deposit remains flat, but a 3-5 mm porous layer must be machined away prior to rolling trials.

Spray Distance and Gas to Metal Ratio

The most sensitive parameters governing the deposition conditions are the spray distance and gas-to-metal (G/M) ratio. Either parameter can be adjusted to change the spray from "wet" to "dry." Generally it is preferred to fix the spray distance and adjust the gas pressure to achieve the desired G/M. Spray distance was varied from 15.5 to 21.2 inches. A nominal distance of 19.5 inches is used for the Tafa unit. This is also in the typical range used by Osprey.

Arguments can be made for shorter spray distances. The strongest is that it is theoretically easier to maintain profile control. However, at shorter spray distances droplet velocities will be higher at impact and the degree of cooling will be less, especially for the larger droplets. Finer sprays could compensate for lower cooling but this will result in higher overspray losses. The effect of droplet velocity on the consolidation behavior of the mushy layer and resulting porosity in the deposit is also unknown at this time. Single droplet experiments at MIT should shed some light on this matter. Also, model designed tests in the Marko unit in which the droplet velocity and drop sizes can be independently varied are planned. A description of these tests is given in Section 1.2.2 below. Further details are given in the Modeling section and by Kozarek et al. (see Appendix I).

Porosity

One of the objectives of the rolling trials is to determine the maximum level of porosity in the as-sprayed deposit which will still produce quality sheet. Bulk porosity typically takes two forms – "Dry" porosity consisting of small ($< 10\ \mu$) irregular pores located at grain boundaries, and "Wet" porosity consisting of larger ($> 20\ \mu$) spherically shaped pores randomly distributed throughout the deposit. Typically these pores are nitrogen filled. Samples representative of low porosity-small pore wet spray, low porosity-large pore wet spray, high porosity-dry spray were selected for the rolling trials. Figures 1.2.2-1.2.5 are photomicrographs showing the as-sprayed porosity representing these conditions.

During the current series of metal spray tests, the potential for hydrogen induced porosity was investigated. Several deposits were analyzed for hydrogen content and showed levels as high as 1.2 ppm. This is significantly higher than ingot cast material. If hydrogen porosity is present it confounds the results of tests to minimize nitrogen porosity. Potential sources of hydrogen are from adsorbed water vapor on the walls of the chamber, residual water in the boron nitride crucible coating, water in the atomizing gas, or absorbed water in various refractory materials inside the chamber. As a result, argon fluxing was added to remove hydrogen from the molten metal charge. After implementing this step, hydrogen levels did not improve, so a vacuum degassing step was added prior to argon fluxing. Measured hydrogen levels still have not improved. There is concern that the analysis procedure is being biased due to interference by other impurities. For instance, because of all the graphite materials presently in the process, a high level of carbides is present. Carbides and other potential interferences are being investigated. Until the analysis issues are resolved we are continuing with the dual degassing steps as a best practice.

Profile

With the Alcoa III nozzle we previously demonstrated the ability to produce a flat deposit. While the purpose to the metal spray runs was to produce deposits for preliminary rolling trials, the nozzle chamber pressures were set to give suitably flat, but not optimized, profiles. All deposits were machined flat prior to rolling. After achieving a suitable number of deposits with a five inch substrate, we made adjustments to increase the spray width to eight inches and to improve the flatness profiles. Following our standard practice the initial nozzle chamber pressures were set according to water spray test data. Chamber pressures were then adjusted for the next run based on the heuristics presented in Section 1.1. Figure 1.2.6 shows the best deposit profile produced during this series of spray trials. This deposit had a 6% standard deviation in thickness. The target flatness for sheet is ± 2%. The next series of runs will focus on optimizing profile. Flat deposits will be required for rolling studies on the as-sprayed deposit.

The optimization studies will require a large number of spray trials if we continue to follow our present procedures. There is a strong need to develop a sensor for measuring deposit shape online which can provide direct feedback for real time nozzle adjustments in the ADU. The need for this capability is reinforced by evidence that the nozzle chamber pressures are changing as the nozzle comes to thermal equilibrium. The magnitude of these changes is

large enough to change the shape of the profile. A feedback control system will ultimately be required to compensate for this phenomena.

The optimization will continue to require extensive use of water spray data to guide pressure settings. Figures 1.2.7 and 1.2.8 compare the results of metal and water spray profiles. Metal spray profiles were generally narrower. Side-to-side asymmetries were generally replicated in each system, however there is a tendency for the Tafa unit profiles to be slightly skewed towards the exhaust port. Numerical models also predict this tendency. Flatness parameters are in fair agreement between water and metal spray tests as shown in Table 1.2.2 below. Flatness is measured as the standard deviation of the normalized deposit thickness over a ±3.1 in. or ±3.8 in. width of the deposit. Thickness measurements are normalized with respect to the deposit cross section so that the sum of the normalized thickness values is unity. This makes the measures independent of actual deposit thickness. The standard deviation of the deposit thickness is generally greater for the metal spray due to the narrowing of the spray relative to water spray.

Table 1.2.2: Comparison of Metal Spray and Water Spray Profiles

	Metal Deposit Profile				Water Spray Profile		
	Run No.	SD +/- 3.1"	SD +/- 3.8"		Run No.*	SD +/- 3.1"	SD +/- 3.8"
	104	0.154	0.0238		78	0.0121	0.0133
	105	0.041	0.051		36	0.03	0.038
	106	0.038	0.042		38	0.038	0.046
	107		0.061		38a		0.046
	108		0.063		38a		0.046
	109		0.064		38a		0.046
	110		0.058		38a		0.046
	111		0.063		38a		0.046
	112						
	113		0.064		38b		0.046
	114		0.061		38b		0.046
	115	0.053	0.066		38b		0.046
	116	0.0054	0.0085		103	0.0071	0.0071
	117	0.014	0.016		98	0.0026	0.0071

*Run 38=nominal; Runs 38a have a higher pressure in Zone 1; Runs 38b have lower pressure in Zone 1 and higher in Zone 2.

1.2.2 Marko Metal Spray Studies

The Marko unit uses a fixed substrate in which a deposit is built up. The process is transient in nature since the deposit thickness and thermal conditions continuously change over the course of the run. The unit has proved useful to determine process conditions prior to committing to a larger scale run in the Tafa unit.

The spray model developed under this program can be used to predict transient spray conditions (liquid fraction, velocity, droplet size, etc.) throughout a run. This model was used to establish a set of Marko unit operating parameters (nozzle pressure, spray distance, melt temperature) which enables prediction of dependent variables such as droplet velocity and size separately.

A designed experiment for 6111 alloy is presently in progress. The test matrix is shown in Figure 1.2.9. Pressure and spray distance conditions are indicated by the circles. Using this technique it is possible to separately examine pressure and distance effects on the deposit structure for the same fraction solid of arriving droplets with small number of runs.

To make this method robust, it requires precise correlations for the nozzle. One goal of the current program at the University of California-Irvine (UCI) is to provide the metal spray droplet size and velocity correlations for the Marko nozzle. Once the data becomes available, designed experiments can be run to elicit the effects of droplet size and velocity on the deposit microstructure.

1.3 Equipment modifications

Several equipment modifications to improve operating efficiency and control on the Tafa spray forming unit are in progress. The first is a major redesign of the melting furnace and delivery system. This change was driven by the need improve operating efficiency for producing deposits for rolling trials. The new furnace system should reduce the manpower requirements as well as provide room for the typical unplanned events. The second modification was to add controls for pressurizing the crucible to provide compensation for the metal head changes during metal spray tests. A third minor modification was to add a Argon purge line for degassing the melt.

1.3.1 Furnace Redesign

The Tafa melting furnace presently uses a graphite crucible with radiant ceramic heaters mounted inside the top section of the spray forming vessel as shown in Figure 1.3.1 The nozzle assembly bolts up to the furnace from below with the connecting drop tube providing the path for metal supply. Turnaround requires the disassembly of the furnace and nozzle equipment every run. The whole crucible disassembly and assembly procedure is time consuming due to the location. The nozzle assembly requires entering the main spray chamber and removing and replacing the nozzle overhead. If there are problems with any of the steps, the turnaround cannot be completed within one day.

The purpose of the redesign is to provide a removable basket assembly containing all the essential elements of the spray forming process -- the crucible, stopper rod assembly, heaters and all electrical connections, insulation, lid, drop tube with the nozzle attached to the underside which can be removed as a unit for service on the bench by a single technician. The unit is shown schematically in Figure 1.3.2.

The removable basket provides a means for more rapid and precise turnaround. It is anticipated the entire procedure can be completed by a single technician with occasional help from a second. The basket assembly with nozzle attached will be lifted out of the top section of the Tafa vessel with a crane and placed on a stand for maintenance. The re-assembled basket assembly will then be repositioned in the Tafa unit guided by alignment pins. Once connections are made, the unit is ready for heat-up.

The unit has been designed and is currently under construction. It will be installed and tested early in the second quarter, 1998.

1.3.2 Crucible Pressure Controls

Crucible pressure controls were added to provide the means to maintain a constant static head independent of the actual level of metal in the crucible. As a result, the flow rate of metal through the nozzle tip can remain nearly constant for the full extent of a spray run. The crucible pressure controls were designed by Air Products.

1.3.3 Degassing for hydrogen removal

A simple metal degassing purge was added to the crucible to assist removal of hydrogen from the melt. The purge consists of a ¼" diameter alumina tube which is immersed in the molten metal. The tube acts as a bubbler through which argon gas is passed. The argon is vented directly to the outside of the vessel through the top of the crucible. In addition to the argon bubbler, degassing is accomplished by slowly drawing a vacuum after melting.

1.4 Thermomechanical Processing and Deposit Characterization

Automotive sheet applications require that porosity be kept to a minimum, a fine recrystallized grain size and sufficient isotropy to eliminate forming problems. The thermomechanical studies included in this project are aimed at developing a rolling practice to produce sheet with the desired characteristics. They will also define characteristics of the as-sprayed deposits needed to achieve the sheet characteristics.

The first set of experiments was designed to identify potential problem areas. Only one deposit was used for this first trial to minimize variation due to differences in starting stock so that we could concentrate on rolling process parameters. Follow-up rolling experiments will use deposits with different porosity characteristics.

The typical process path for the production of sheet begins with hot rolling ingot to an intermediate gage. In some instances the hot rolled intermediate gage is annealed before cold rolling. After cold rolling to final gage, the sheet is coiled and sent to a continuous temper line for heat treating.

1.4.1 Rolling and Heat Treating

A single spray deposit was sawed and machined to yield two pieces of rolling stock; one 0.250 x 2.5 x 16 in. (A) and one 0.340 x 2.5 x 16 in. (B). Both the top and the bottom surfaces of the deposits were machined. To maximize recovery from each section of the deposit, the two pieces were machined to different thickness. The spray conditions used for this deposit are listed in Table 1.4.1. Figure 1.4.1 is a photograph of a typical as-sprayed deposit.

Table 1.4.1 Spray Parameters for 6111 Rolling and Characterization Studies

Sample ID	A / B	C
Run Number	109	115
Nozzle	Alcoa III	Alcoa III
Gas Slit	0.040 in.	0.040 in.
Alloy	6111	6111
Melt Superheat	350°F	350°F
Spray Distance	19.5"	19.5"
G/M	1.02	1.17
Substrate Speed	120 in/min	100 in/min
Substrate Width	5"	5"
Substrate Material	S S	S S

Rapid heating to the rolling temperature is desired to simulate commercial spray forming conditions in which deposits are rolled immediately after solidification and to minimize dissolution and precipitation of soluble second phase particles. Infrared heating was, therefore, selected instead of air furnace heating. A single hot roll reduction pass was used for each deposit. Deposit **A** was hot rolled to 0.125 inch while **B** was hot rolled to 0.111 inch. The plates were still air cooled after rolling.

To evaluate the effect of an anneal on grain structure and texture, half of each sheet sample was annealed before cold rolling both halves. Samples of both the annealed (**AY**) and non-annealed (**AN**) hot rolled sheet were cold rolled to various gages.

Solution heat treat study

Under production conditions, coiled sheet is usually solution heat treated in a continuous heat treating line where it is uncoiled, passed through an inline heat treating furnace, quenched and recoiled. The line speed is determined by the time required for dissolution. A solution heat treat study was performed to evaluate the influence of rolling conditions and hot line gage anneal on dissolution time.

Cold rolled sheet samples, **AY** and **AN**, 0.036 inch thick, were used to evaluate the time required for dissolution during solution heat treatment. The samples were heated, held for a variable number of seconds and then cold water quenched. The electrical conductivity of each sample was measured immediately after quenching and measured again several times a few seconds later. Electrical conductivity provides a semi-quantitative measure of how much solid has gone into solution. Results suggest that there is negligible change in conductivity as a function of time at temperature. However, the scatter in the data also indicates that the sensitivity of the conductivity measurements may not be sufficient to discern differences between the samples. Further experiments will be needed.

1.4.2 Metallographic Evaluations

As-sprayed

The as-sprayed 6111 deposits produced in the Tafa unit under normal spray conditions, typically, have fine equiaxed grains (Figure 1.4.2). The grain size ranges from 10 to 50 μ (Figure 1.4.3). This grain size is much finer than that normally observed in conventionally cast 6111 alloy ingot (400 μ).

The spray deposits are relatively dense compared with typical 3003 spray deposits sprayed earlier in the DOE program [4]. As with 3003, two types of porosity were observed. Base porosity at the substrate-deposit interface typically has a thickness of about 3 mm. The bulk porosity varies depending on the spray conditions. Porosity shown in Figure 1.4.4 for deposit **C** has a fine and irregular shape and is typical of a "dry" or "cold" spray. With this type of porosity, the volume fraction of bulk porosity is low. Also, since this type of porosity is believed to result from shrinkage, gas is not normally entrapped in the pores of dry sprayed deposit. Thus the pores are expected to be healed during subsequent fabrication into finished product. The 6111 spray deposits contain very fine constituent particles--less than 2 μ. A fine constituent particle size is expected to improve the ductility of the final product.

The grain microstructure of deposits **A & B** before hot rolling is shown in Figure 1.4.5. Grains are fine and equiaxed. Bulk porosity is rounded in shape, with some of the pores as large as 125 μ, indicating hotter spray conditions than in Figure 1.4.4. Large pores of this type are believed to result from entrapped gas – either nitrogen or hydrogen. It may be difficult to heal the larger pores during the hot rolling step. A major activity for the next period will be to

determine what level of porosity (size, concentration and type) can be healed during rolling operations.

After hot rolling

Samples of hot rolled sheet were examined to determine the distribution of second phase particles and look for the presence of porosity and inclusions. The hot rolled samples were given a simulated coil cool. Selected samples were also given a full anneal. Figure 1.4.6 shows second phase particles to be fine and uniformly distributed in both annealed and unannealed samples. The majority of the constituent particles are smaller than 5 μm. In contrast, constituent particle size in typical ingot is 10-20 μm. Precipitate particles containing Mg and Si are also very fine; less that 1 μm. These particles may have coarsened slightly during the anneal as is expected.

Some relatively large inclusions were observed in a few of the samples. Microprobe analysis was used to identify an inclusion that was observed optically (Figure 1.4.7). These inclusions contain magnesium, silicon and oxygen and are typical of spinels that form during melting operations. These are typically removed during downstream metal processing operations through settling and/or filtering. Metal is not filtered in the Tafa spray forming unit prior to spraying. The ADU will include a filtration step.

Samples of the hot rolled plate were electro etched and viewed using polarized light to reveal the grain structure. Representative photomicrographs are shown in Figures 1.4.8 and 1.4.9. The annealed samples (Figure 1.4.10) are fully recrystallized with a grain size of 20-150 μ. The grain size of the sheet increased with increased rolling. This is the reverse of what is expected. Possible explanations may include grain growth during the anneal. The samples that were not annealed (Figure 1.4.9) appear to be unrecrystallized.

After cold rolling

Following cold rolling the samples were solution heat treated. Samples for W-temper metallographic evaluation were heated and cold water quenched. To reveal features of porosity, inclusions, dispersoids and graining structure, samples were evaluated in the as-polished condition, after etching with 0.5% HF and after electro etching.

Solution heat treating is performed to put all the solute into solid solution. Comparison of Figure 1.4.10 with Figure 1.4.6 suggests that the solution heat treatment was effective. That is, only constituent particles are present in the solution heat treated samples. Furthermore, there is little difference between annealed an non-annealed samples.

After electro etching, samples were viewed under polarized light to reveal the grain structure (Figure 1.4.11). All of the cold rolled sheet was fully recrystallized with 20-100 μ grains. The recrystallized grain size is larger when hot rolled sheet was annealed before cold rolling than when the hot rolled sheet was cold rolled directly. The grain size of commercial 6111 produced from ingot is typically 50-100 μ.

1.4.3 Texture Evaluations

When metal is deformed by rolling or other processes, grains acquire a preferred orientation or texture. That is, a certain percentage of grains rotate to an ideal orientation with the others scattering to random orientations. Often, several ideal orientations coexist. This mix of orientation distributions describes the deformation texture. When the metal is heated, as in annealing or solution heat treating, the material can acquire a new texture. X-ray diffraction is used to measure the orientation of grains in samples with respect to a reference location.

X-ray diffraction was used to measure the texture of 6111 sheet produced from deposit A under various treatments. Table 1.4.2 lists the percent of each texture component in each sample. Both samples exhibit a very weak texture and there is little difference between the samples. A weak texture is desired for most forming operations.

Table 1.4.2

Texture Components
6111, 0.036 inch Sheet

	Component Fraction, %	
Texture Component	739762-AY Annealed Before Cold Rolling	739762-AN No Anneal Before Cold Rolling
Brass	0.00	0.00
Beta 2	0.00	0.00
Beta 3	0.65	0.26
S	0.51	0.38
Beta 4	0.56	0.38
Beta 5	0.96	0.91
Copper	2.40	1.91
Cube	3.30	4.20
Goss	1.14	0.00
Nd Cube	0.00	2.88
P	0.48	0.00
Other	90.0	89.08

1.5 Modeling

1.5.1 Modification of the Spray Simulation Code

Established Simulation Capabilities

For the spray forming process development, we developed a rigorous approach for modeling the spray process by a three-dimensional numerical simulation which solves simultaneously the coupled, transport equations of both dispersed droplets and continuous gas flow using a tracking or Eulerian-Lagrangian approach. Results obtained from the study showed favorable agreement with the available test data.

The computational model was developed based on the mathematical formulations for the transport phenomena inside the chamber. The computational code for solving the associated mathematical models were developed jointly with our subcontractor, Professor M. K. Chyu

of Carnegie Mellon University (CMU). The first phase of the code development was completed and was concentrated at modeling the specific geometry associated with the Tafa spray chamber used at the Alcoa Technical Center.

Here is a brief description to recapture some important features of the spray simulation model. The spray is a two-phase flow where there are interchanges of momentum and energy between the gas and the metal droplets. The convective transport of gas phase is governed by Navier-Stokes equations combined with a two-equation k-ε turbulence model. The mathematical formulations and the numerical model developed represent the conservation principle of mass, momentum, enthalpy, turbulent kinetic energy, and the dissipation rate of turbulent kinetic energy for unsteady, compressible turbulent flow. In the formulations, interactions of gas with dispersed droplets are accounted for. Variation of gas density and viscosity with temperature is governed by the equation of state. For the droplets, the momentum balance equation along with the heat balance equation are solved for tracking the velocity and temperature of the droplets. For the droplet solidification, a liquid droplet has to pass through five successive thermal regions before complete solidification is achieved. The five thermal regions are: convective cooling in liquid state, nucleation and recalescence, segregated solidification, eutectic solidification, and cooling in the solid state, respectively. The temperature histogram for aluminum is programmed into the computer code.

In an actual spray, millions of droplets co-exist within the spray chamber. Current computing power remains incapable of tracking each individual droplet. As a common practice, a relatively small number of computational droplets, each representing a group of real world droplets having the same properties (e.g., size, velocity, location and temperature) are sampled to represent all droplets. The sampling procedure uses the Monte Carlo technique. Injection droplet size, velocity, and gas-turbulent-fluctuation velocity are all determined by the same stochastic procedure.

The three-dimensional spray simulation model is a custom-developed, finite-volume, computational fluid dynamics code. The computation includes iterative procedures for gas flow solution, droplet tracking, temperature calculation, and solidification modeling. Results obtained reveal important process information such as droplet distribution, velocity, temperature, fraction of solidification, preform shape, and chamber effect.

Modified Simulation Capabilities

The simulation model developed in prior work focused on a cylindrical geometry used for the Tafa spray chamber [4]. For the next phase of spray forming development work, an Advanced Development Unit (ADU) is being designed and developed. The features involved in the ADU will be much different than those in the bench scale unit. Here are two examples:

- The shape of the ADU will be more rectangular and scalable as nozzle width increases with sub-chambers that can be easily put together as modules.
- In the ADU, there will be additions of gas flow baffle/shrouding devices to customize the gas-droplet flow pattern for process optimization.

In addition to numerical modeling, more water spray experiments are being planned to further assist the spray nozzle design work. Hence there is a need to apply the simulation model into water spray calculation to enhance the value of the water spray testing. With both water and metal simulation work we can more effectively develop the correlation to assist the process design.

The spray simulation code is being modified to deliver the capability to address the needs for ADU development work as well as the water spray experiments. Specifically, they are:

- Adding the capability for simulating water spray.
- Assisting ADU chamber design work.
- Modifying the chamber shape to closely resemble the final ADU design.
- Adding user friendly features for running the code, particularly on shape and meshes.

The mathematical formulations involved remain unchanged. The material properties for water have been added, and the shape of the chamber has been changed to a rectangular type. The code is being tested for a simplified chamber geometry.

Preliminary simulation results on the deposit profile from water spray in a simplified rectangular chamber are as shown in Figures 1.5.1-1.5.3. Figure 1.5.1 shows the three-dimensional deposit profile distribution on a fixed flat substrate (in shaded form). The same profiles in a surface perimeter form are shown in Figure 1.5.2. Figure 1.5.3 shows the effect of reducing chamber size.

1.5.2 Deposit Thermal Model for Marko Spray Unit

A two-dimensional transient thermal model was developed to simulate the thermal history of a deposit as a result of spray in the Marko spray unit. The model is a useful tool to study the influence of process parameters on the formation of porosity. The model was used to assist the design of experiments to find the operating windows for minimizing porosity in the bulk. A brief description of the mathematical model as well as the integration of modeling technology with experimentation is given.

For the linear shaped spray process, we found through modeling that the location of the transition between the base and bulk porosity in a deposit can be closely related to the thermal behavior of the deposit during the spray process. A two-dimensional transient thermal model was previously developed to help determine the location. The work was reported earlier by Pien, et al. [7]. In this work, we developed the model for the application of the Marko spray unit in which conical-shaped deposits are produced.

The transient two-dimensional thermal model predicts the thermal history of the deposit and the substrate system. From the temperature solutions, we can study the formation of mushy layer on the top of metal surface, its thickness and the relation to the deposit results. Figure 1.5.4 shows the schematic drawing of the problem under study and the associated radial coordinates system for the mathematical formulation and the numerical formulation.

The thermal physical properties of the materials for both deposit and substrate are assumed constant, independent of temperature. They include density, specific heat and thermal conductivity. The effect of temperature on these properties can be added in the future if more detailed simulation of the problem is required.

The mass flux distribution of metal at radius r for a round nozzle can be described, in general, by the following equation:

$$\dot{m}(r) = \dot{m}_c \bullet \exp\left[-k_1\left(\frac{r}{R}\right)^{k_2}\right] \qquad (1)$$

where $\dot{m}_c$ is the mass flux of the metal spray at the center of the deposit and R is the characteristic radius where $\dot{m}(r) / \dot{m}_c = 0.5$. Hence, R's value depends on the development of the spray tent. The two constants involved in the equation are: $k_1 = \ln(2)$ and k_2 is a characteristic constant whose value depends on the nozzle design. Both values of R and k_2 can be estimated by using the results obtained from our spray simulation model previously developed to simulate the three-dimensional transport phenomena of the two-phase system containing gas and droplets [7,9,10].

With the mass distribution of the spray being described by Equation (1), the transient development of the height of the deposit in the radial direction can be modeled as:

$$Z(r,t) = \frac{\dot{m}_c}{\rho_d} t \bullet \exp\left[-k_1 \left(\frac{r}{R} \right)^{k_2} \right] \qquad (2)$$

where t is time and ρ_d is the density of the deposit (metal).

The deposit is formed by accumulating metal droplets in the spray tent which arrive at the top surface of the deposit. The averaged temperature of the metal is likely to be in the mushy range which could move downward along the inclined surface. However, for the simplicity purpose of the modeling, we assume that no downward flow is involved. This could be a reasonable compromise considering the fact that for an optimal spray operation, it is desirable not to maintain a thick layer of liquid-like metal on the top of the deposit surface so that bulk porosity can be reduced.

Spray Model

Predicting temperature profiles requires reliable information on the characteristics of the spray such as spray mass distribution and enthalpy of the metal droplets in the spray tent. A full-scaled spray simulation model, which was previously developed at ATC [1,3,4], can be used to predict the needed information. The spray model is capable of simulating the transport phenomena occurred in the spray forming process and determines the thermal histories and velocities of the gas and metal droplets in the spray chamber.

Figure 1.5.5 shows a schematic diagram for the input and output of the spray model. The main body of the spray model simultaneously solves the coupled, transport equations of both dispersed droplets and continuous gas flow. A combined Eulerian-Lagrangian approach is formulated treating droplets as discrete entities in a continuous gas field described with an Eulerian framework. The governing equation as well as the basis of the physical models implemented in the numerical model was described previously [3].

The gas pressure is the major input process variable. We used a Lubanska type correlation [10] to estimate the effects of pressure on droplet size distribution for the nozzle used in this study. By combining the spray model with the deposition model described in this report, we can calculate the thermal behavior of the deposit during the spray forming process.

Model Assisted Design of Experiments

The experiment was to determine how the liquid fraction of the metal spray arriving at the deposit controls the level of bulk porosity. A series of calculations was made using the spray model to determine the process conditions which will yield a given average liquid fraction in the droplets arriving the substrate. The independent process parameters were the atomizing gas pressure and flight distance. Based on the spray model calculations, a test matrix was set up to examine the effects of spraying at four levels of liquid fraction obtained by using several levels of the atomizing gas pressure and flight distance. By using the model, it was possible to select test conditions in which the liquid fraction could be held constant while the independent parameters were varied at several levels. This experimental design allows us to test the effects of pressure and distance on porosity in the deposit.

Experiments were performed for selected cases. The description of the experimental work and the results on the measurement of the porosity were reported earlier [5]. Following, we will highlight the results of modeling computation and compare them to those measured experimentally.

Modeling Results

The finite-difference equations for the temperatures of the deposit and the substrate are solved numerically. Figure 1.5.6 shows computed location of the top surface and the solidus isotherm vs. spray time at a fraction of solid of 0.6. Between the top surface and the solidus location the metal is in the mushy state. This figure clearly shows that after a deposit reaches

a threshold thickness, the mushy layer thickness grows rapidly as the spray continues. The experimental results also suggest that such a growth of mushy layer thickness exists [5].

Figure 1.5.6 also shows that for the deposit region within the critical deposit height near the substrate, the temperature of the deposit for the whole region is less than the solidus temperature. This indicates that in this region the metal droplets solidify almost instantaneously upon their arriving at the top layer of the deposit. The porosity formed in this region is therefore characteristically different ("dry" porosity) than that formed in the upper region of the deposit where a mushy layer exists ("wet" porosity). Figure 1.5.6 therefore plots the measured locations of the "dry" to "wet" transition point taken from the porosity measurement of the test samples and compares them with the calculated threshold results. As shown, the calculated results compare reasonably well with the measured ones.

2.0 ADVANCED DEVELOPMENT UNIT DESIGN AND CONSTRUCTION

With the overall reduction in program scope, Alcoa has modified the technical approach to address key technical/commercialization issues prior to committing to the construction of an Advanced Development Unit (ADU). While the construction of the unit has been postponed, work continues on design concepts and collecting information for critical and/or long lead time elements of the ADU. During this period work was performed on the Melt Delivery Module, design of the Chamber Module, and the process control system.

2.1 Metal Delivery Module

A key requirement for the melt delivery module is to provide a constant (but adjustable) supply of metal to the nozzle. In-line filtering and de-gassing are required for metal quality. The system will consist of a fixed melting furnace, a pressurized lid, removable transfer tube, transfer trough, and a tundish. After metal is melted, the furnace will be sealed and pressurized to force metal from the bottom of the crucible up through the transfer tube and into the trough. The trough will convey the metal to the tundish where it will empty into the spray nozzle. Preliminary tests have shown positive results.

2.2 Spray Chamber Design

Earlier modeling work has shown that the chamber shape is tightly coupled to the gas flow patterns and the resultant deposit shape. The approach we are taking is to design the chamber shape based on the gas flow dynamics and later test these designs using a physical model.

Work is underway to construct a complete math model of a rectangular geometry spray chamber. This was described in the previous section on modeling.

2.3 Process Control System

Design work on the control system has been limited to the melt delivery system. Testing of the previously mentioned method of controlling the supply of metal to the nozzle has resulted in a robust control system that can accurately discharge and regulate flow from the furnace to a tundish. This system, in combination with tundish level control, is able to sufficiently maintain static head pressure at the nozzle.

The computer equipment used to provide control of melt delivery can also form the core of an overall process control system. As a result, all aspects of the process can be controlled in a single, tightly integrated system at minimal cost. Functions of the system will include real time control of process parameters, data acquisition, information storage, video capture, and operator interface.

3.0 DEVELOP ADVANCED DEVEVELOPMENT UNIT PROCESS CONDITIONS

No work was performed on this task this period.

4.0 ECONOMIC ANALYSIS

No new data was generated to update the investment analysis.

5.0 PROJECT MANAGEMENT

5.1 Agreements

Metals Initiative Holding Company Agreement #DE-GM07-98ID11353 was incorporated into Amendment #M007 of the Alcoa/DOE Cooperative Agreement, dated December, 1997. The agreement establishes ownership of intellectual property rights developed under the program, filing and licensing requirements, costs and royalties, and the repayment of government contributions. In addition it establishes the industrial participants in the Holding Company.

Concurrent with this, Alcoa entered discussions with the DOE to establish an ownership position for intellectual property developed outside of the Cooperative Agreement. Amendment #A006 of the Alcoa/DOE Cooperative Agreement, dated September, 1997 incorporated a new paragraph (12.d) which develops an understanding of work and areas of research conducted under the DOE supported Spray Forming Program and a simultaneously conducted Alcoa privately funded research project. The final wording of this paragraph is still under discussion, and will be the subject of a future amendment.

5.2 Subcontracts

There were six subcontracts issued during the reporting period. Following are the statements of work for each subcontractor:

1. Dr. M. K. Chyu - Carnegie Mellon University

   Subrecipient shall conduct the research program per the attached proposal entitled "Modeling of Spray Forming Process: Droplet-Substrate Interaction and Near Wall Heat Transfer," dated December 15, 1996 as follows:

   A. Three phenomena to be modeled:
      1. Thermal condition of droplets in flight and at impact on substrate.
      2. Temperature distribution at substrate.
      3. Effect of chamber design on gas and droplet flow.
   B. Physical configurations to be modeled will be specified by Alcoa.
   C. All code developed must run on Alcoa systems.

2. Dr. T. I-P. Shih - Carnegie Mellon University

   Subrecipient shall conduct the research program per the attached proposal entitled "Effects of Nozzle/Baffle Design on Spray Depositions," as follows:

   A. Perform 2-D and 3-D calculations on nozzle systems.
   B. Characterize effect of nozzle configuration and operation on final deposit.
   C. Physical configurations to be modeled will be specified by Alcoa.
   D. All code developed must run on Alcoa system.

3. Dr. R. D. Doherty - Drexel University

   Subrecipient shall consult and assist Company to achieve an improved understanding of the mechanical processing of spray formed sheet materials as follows:

   A. Consultant in developing a TMP path for 6111 sheet alloy including:
      1. Analysis of cast structure.
      2. Preheat and rolling schedule.
      3. Solution heat treat and quench path.
      4. Aging schedule.
   B. Consultant on analysis of final structure and mechanical properties.

4. University of California-Irvine

   Dr. Enrique Lavernia shall conduct the research program per the attached University of California-Irvine proposal dated January 30, 1997 as follows:

   A. Spray plume characterization - perform particle size distribution and velocity measurements, using Alcoa's PDPA, focusing on the Alcoa-provided circular nozzle.
   B. Analysis of process/structure relationships to determine effect of particle and velocity distribution on deposit microstructure.

5. Massachusetts Institute of Technology

   Dr. M. Flemings shall conduct the research program per the attached MIT proposal dated September 23, 1996 as follows:

   A. Measure undercooling behavior of 6111 droplets.
   B. Characterize Structure of solidifying 6111 droplets.
   C. Analyze effect of process conditions on microstructure.

6. Massachusetts Institute of Technology

Dr. J. H. Chun shall conduct the research program per the attached MIT proposal dated October 11, 1996 as follows:

A. Selection of aluminum alloys, substrate materials and droplet impact conditions in consultation with Alcoa Staff.

B. Characterization of droplet and deposit thermal states as a function of the processing parameters.

C. Design and testing of experimental schemes to study the impact behavior under various droplet and deposit conditions.

D. Visualization of the droplet impact behavior using a Kodak Ektapro high speed video camera system in collaboration with Sandia National Laboratories.

E. Analysis of experimental data.

Technology Transfer

During the period, the following papers and presentations were made:

- A. Mansour, N. Chigier, T. Shih, R. L. Kozarek, *The effects of the Hartman Cavity on the Performance of the USGA Nozzle used for Aluminum Spray Forming*, Atomization and Sprays, Volume 8, Number 1, January-February, 1998.
- Y. Zhou, S. Lee, V. McDonnell, S. Samuelson, R. L. Kozarek, and E. Lavernia, *Influence of Operating Variables on Average Droplet Size During Linear Atomization*, Accepted for publication in Met Trans B, 1998.
- J. E. Fischer, R. L. Kozarek, *A Probe to Measure the Particle Enthalpy at Impact During the Spray Forming Process*, Solidification 1998, Proceedings of Solidification and Deposition of Molten Metal Droplets Session, edited by S. P. Marsh, et al., TMS Annual Conference, February, 1998.
- R. L. Kozarek, M. G. Chu, S. J. Pien, *An Approach to Minimize Porosity in Spray Formed Deposits Through a Model-Based Design Experiment*, Solidification 1998, Proceedings of Solidification and Deposition of Molten Metal Droplets Session, edited by S. P. Marsh, et al., TMS Annual Conference, February, 1998.
- S. J. Pien, "Modeling of Spray Forming Process," presentation at Solidification 1998, TMS Annual Conference, San Antonio, TX, February, 1998.

In addition the following patents and invention records were submitted:

Patents:

- *A Linear Nozzle with Tailored Gas Plumes and Method*, USSN 08/915,230.

Invention Reports:

- None for the reporting period.

6.0 REFERENCES

[1] R. L. Kozarek, Spray Forming Aluminum - Second Annual Report (Phase II) September, 1997, Alcoa Report No. C97-38411-R2.

[2] W. DuBroff, "Development of Sprayforming process for Steel," Final Program Report, U. S. Department of Energy, December 1991.

[3] R. L. Kozarek, Spray Forming Aluminum - Annual Report (Phase II), Technical Progress, 1997 March, Alcoa Report No. C97-38411-R1.

[4] R. L. Kozarek - Private Communication with A. Ogilvy - Osprey Metal Ltd., Neath, Wales, U.K.

[5] R. L. Kozarek, M. G. Chu, S. J. Pien, *An Approach to Minimize Porosity in Spray Formed Deposits Through a Model-Based Design Experiment*, Solidification 1998, Proceedings of Solidification and Deposition of Molten Metal Droplets Session, edited by S. P. Marsh, et al, TMS Annual Conference, February, 1998. [Alcoa Funded Work]

[6] S. J. Pien, M. K. Chyu and H. Ding, "Modeling of the Multi-Phase Transport Phenomena and Solidification in a Spray Forming Process with a Linear Nozzle," Proceedings of the 3rd International Conference on Spray Forming, pp. 45-52, Cardiff, UK, September (1996).

[7] Osprey technical document "The Osprey Know-How" by the Osprey Metals Ltd.

[8] S. J. Pien, "Modeling of Spray Forming Process," Alcoa Technical Center Report No. 46-94-005-10M006, Alcoa Technical Center, Alcoa Center, PA 15069 (1994).

[9] M. K. Chyu, H. Ding, S. J. Pien, and J. Luo, 1995, "Modeling of Droplet Flow, Temperature and Solidification in a Spray Forming Process," HTD-Vol. 317-2, Proceedings of ASME Heat Transfer Division, Vol. 2, pp. 371-380 (1995)

[10] H. Lubanska, "Correlation of Spray Ring Data for Gas Atomization of Liquid Metals," J. Metals, p. 45, February 1970.

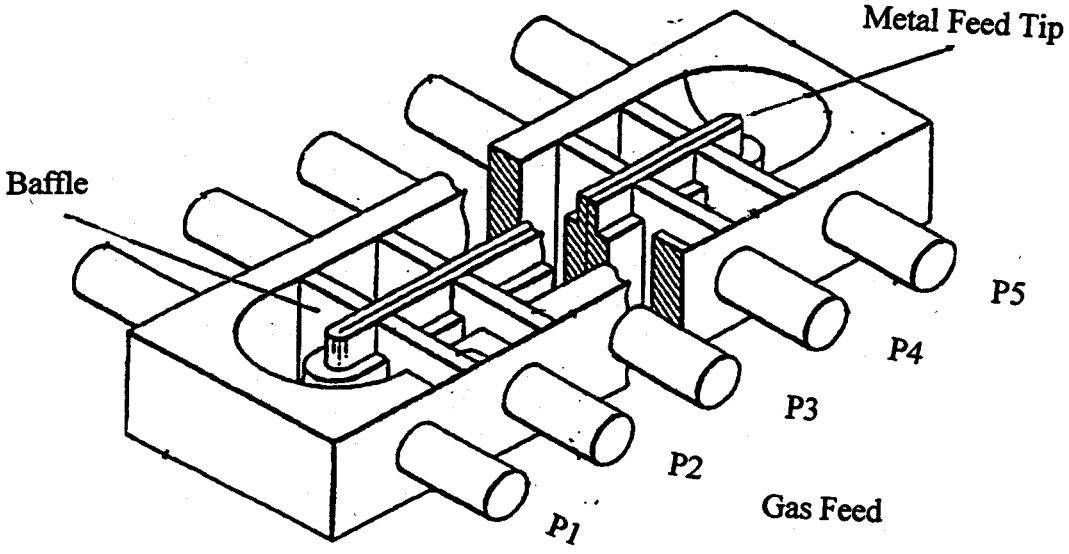

Figure 1.1.1: Cutaway schematic of Alcoa III nozzle

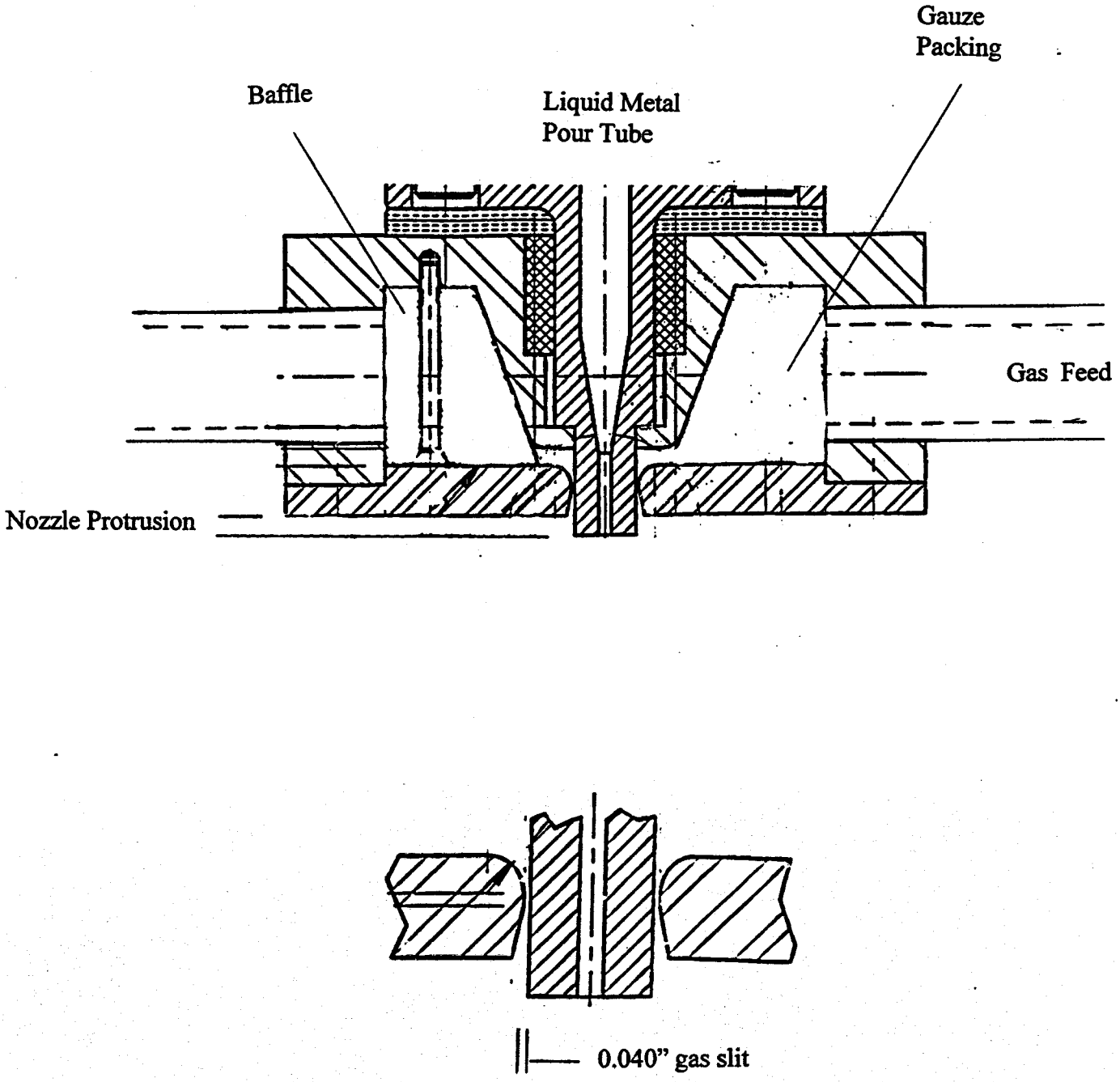

Figure 1.1.2: Transverse section of Alcoa III nozzle illustrating gas slit geometry.

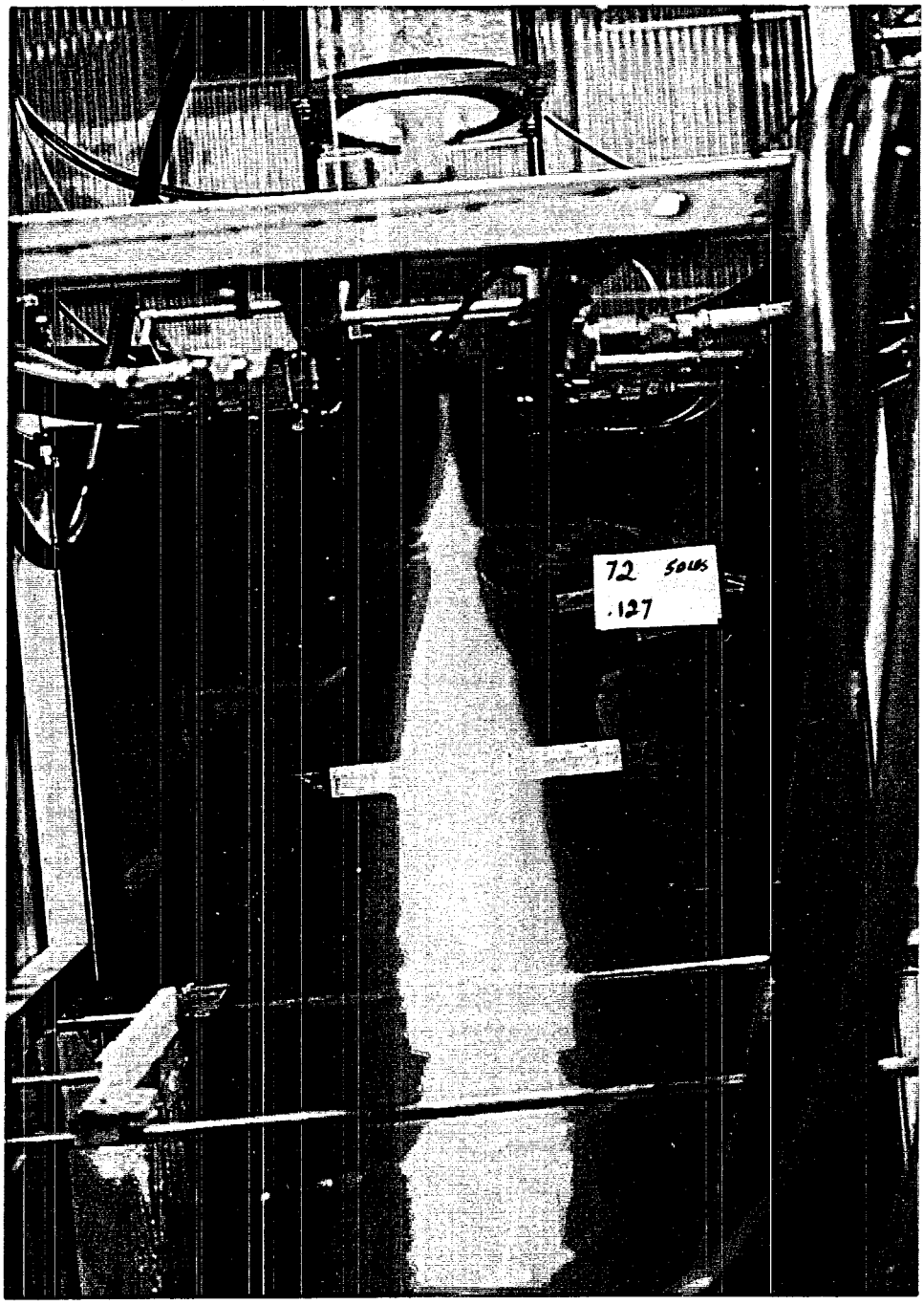

Figure 1.1.3: Photograph of test stand and patternator

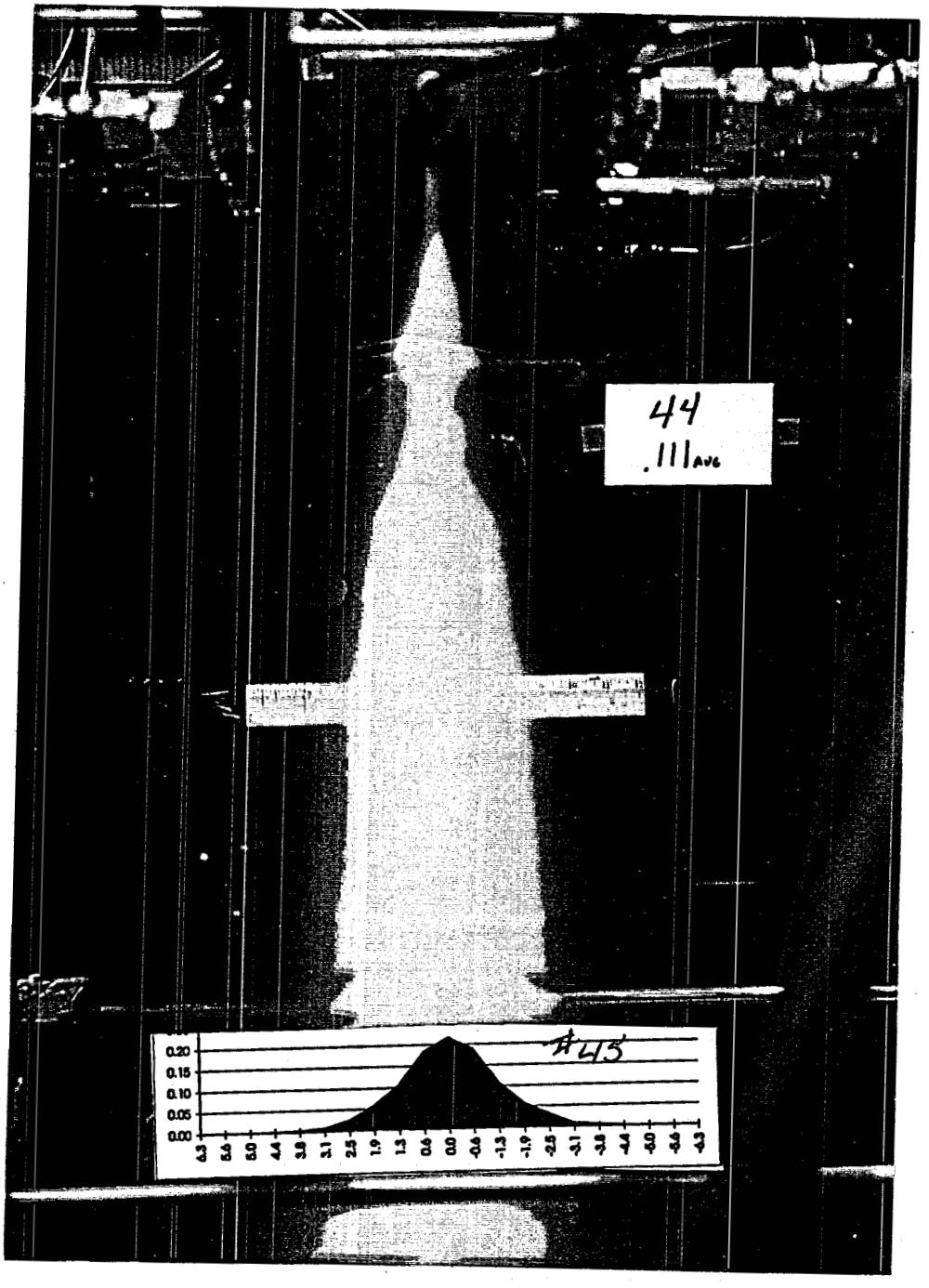

Figure 1.1.4 Photograph and mass flux profile of short axis water spray

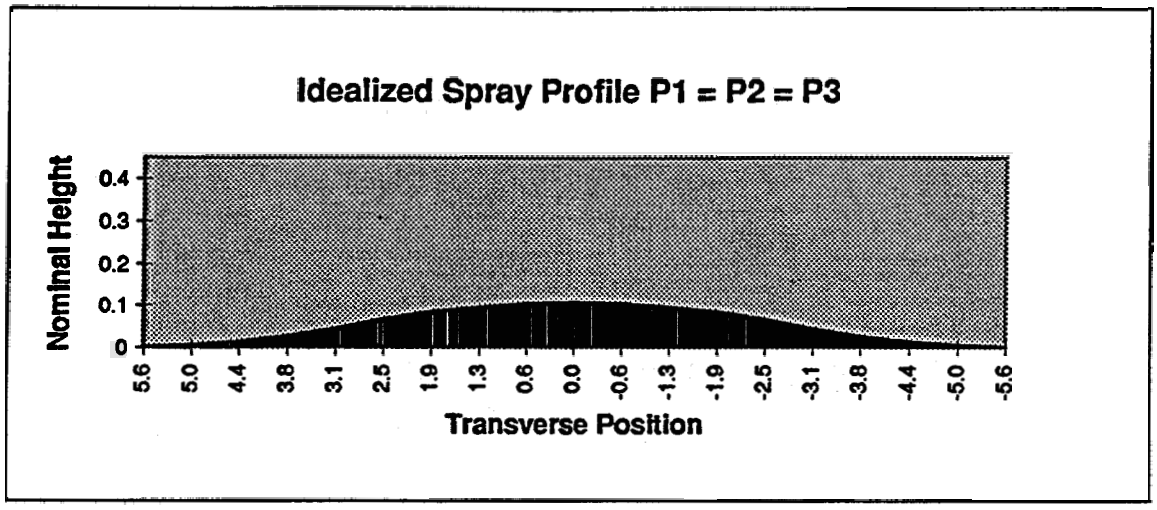

Figure 1.1.5

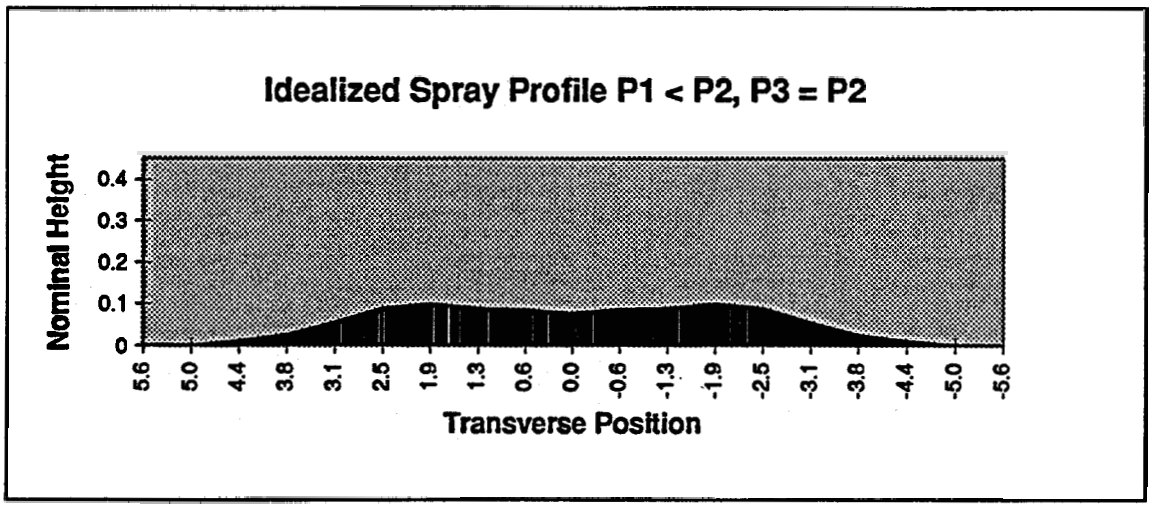

Figure 1.1.6

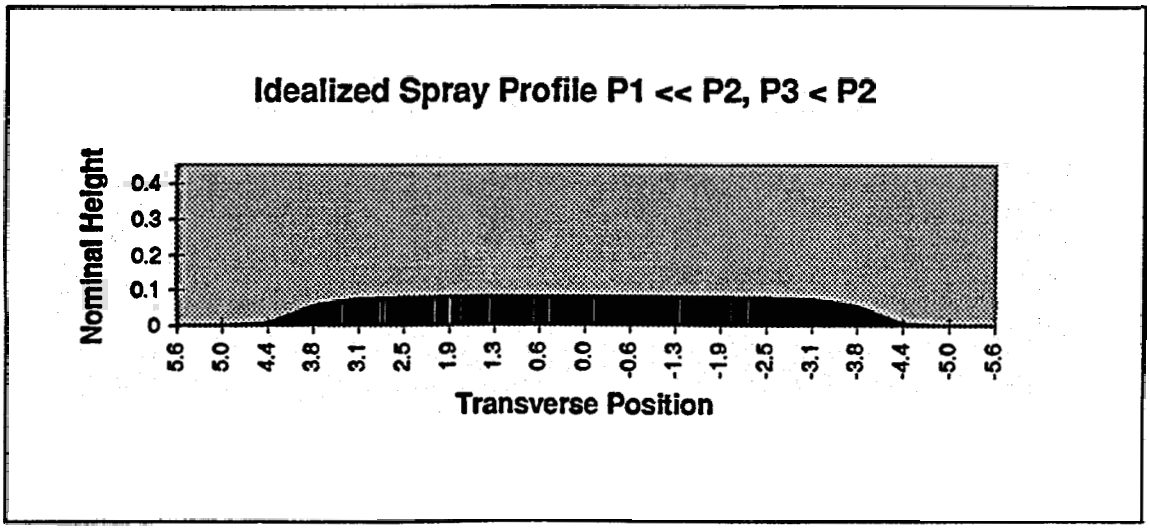

Figure 1.1.7

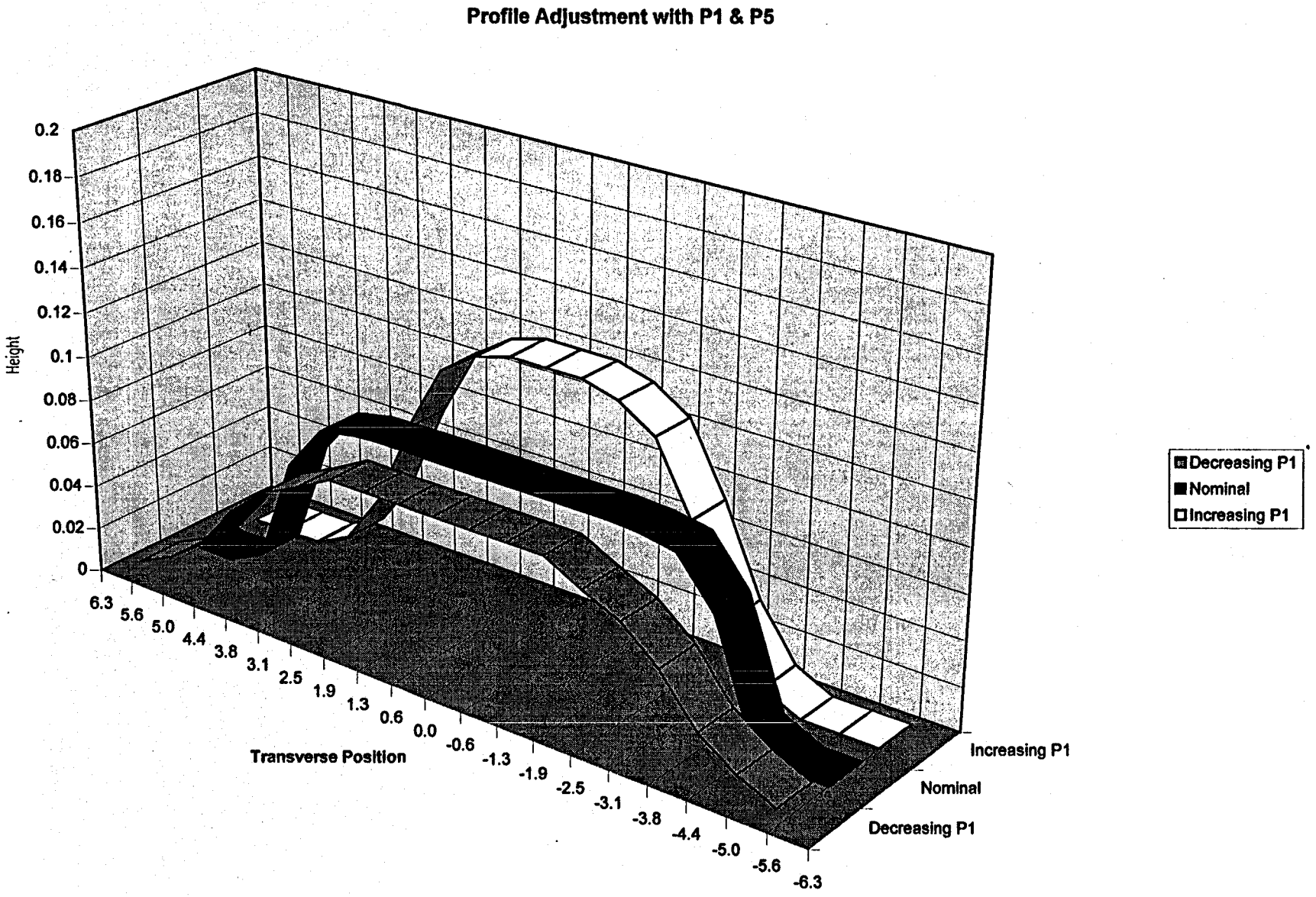

Figure 1.1.8 Effect of changing P1 on Idealized profile

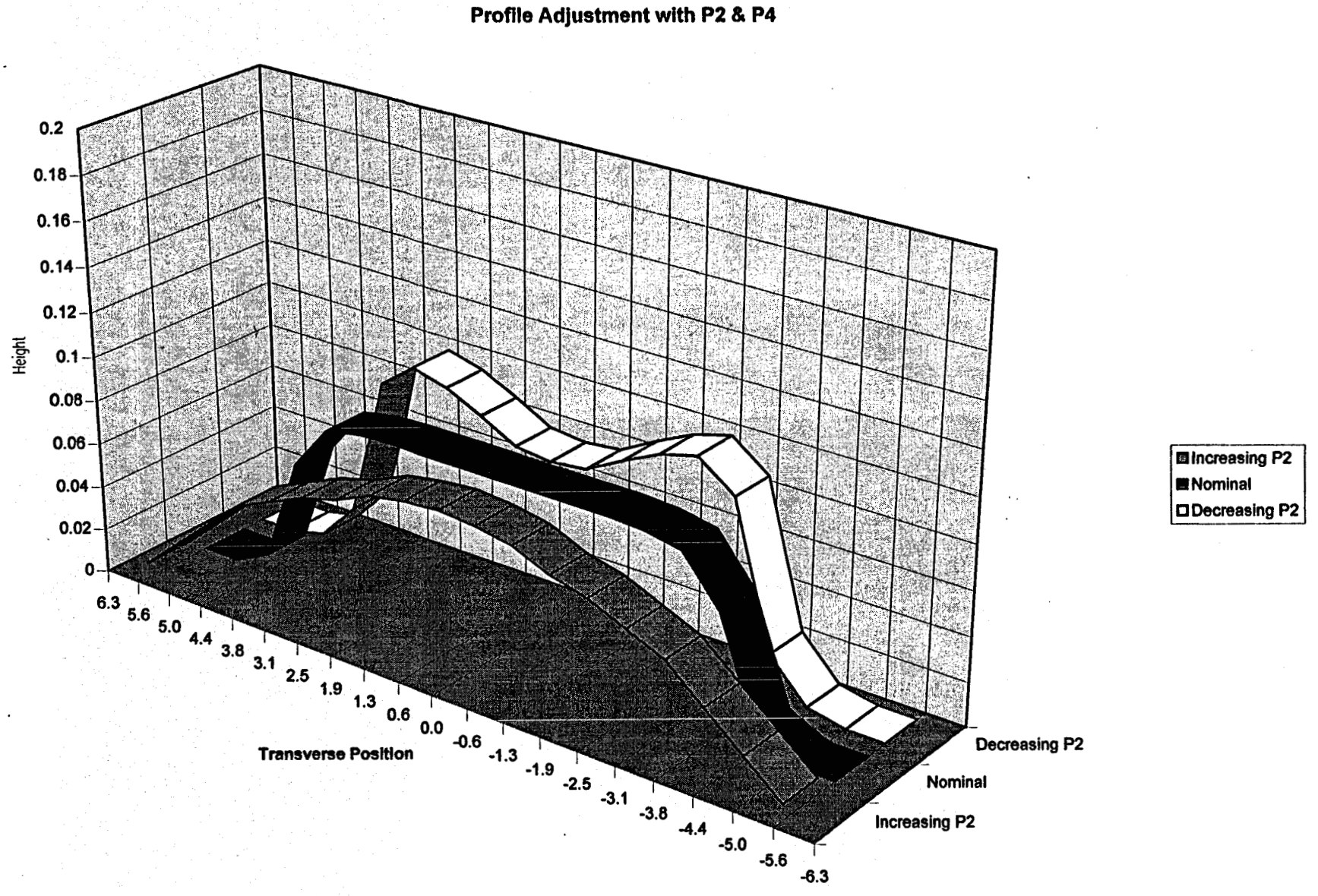

Figure 1.1.9 Effect of changing P2 on Idealized profile

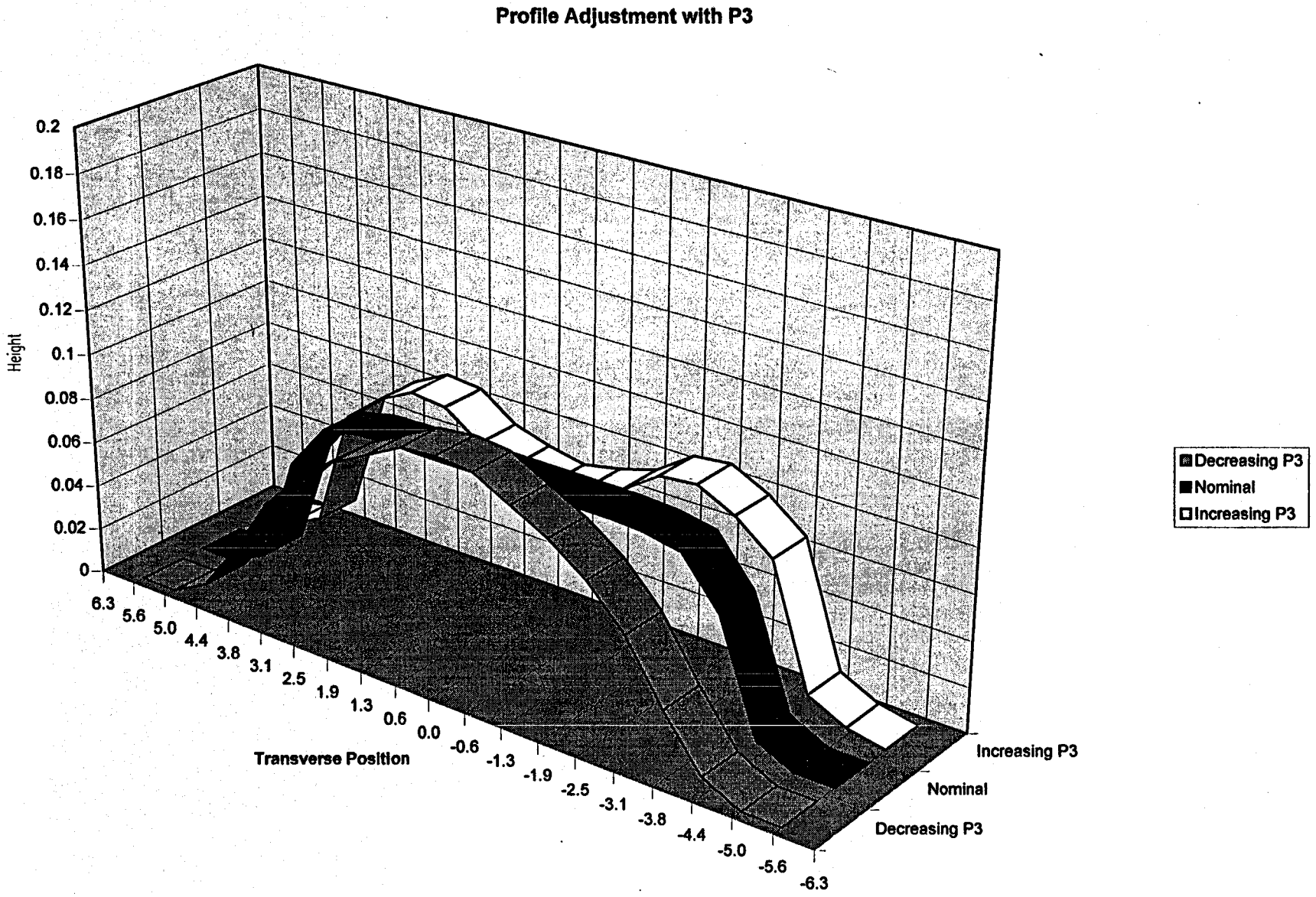

Figure 1.1.10 Effect of changing P3 on Idealized profile

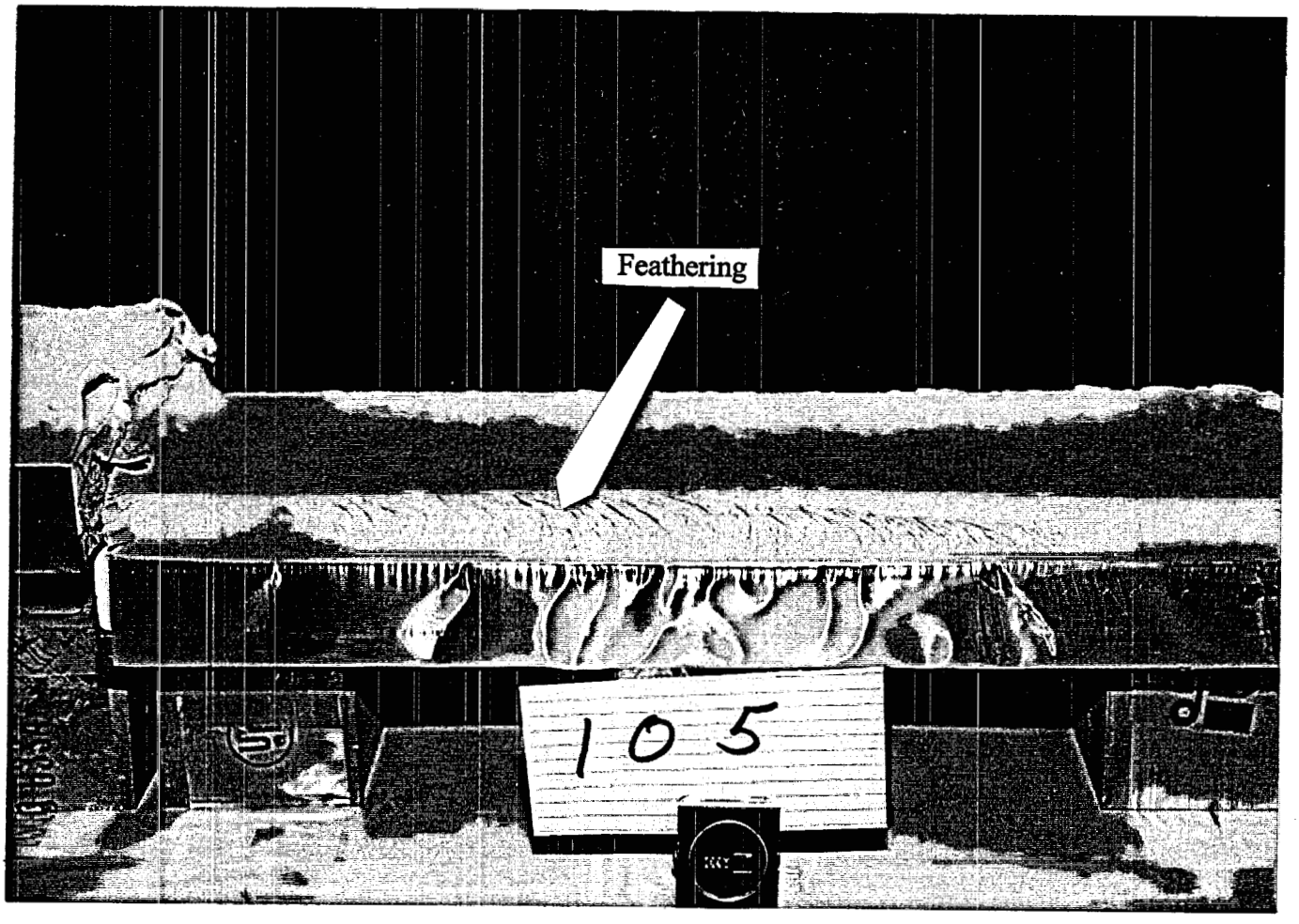

Figure 1.2.1: Photograph of a 6111 alloy deposit illustrating "feathering"

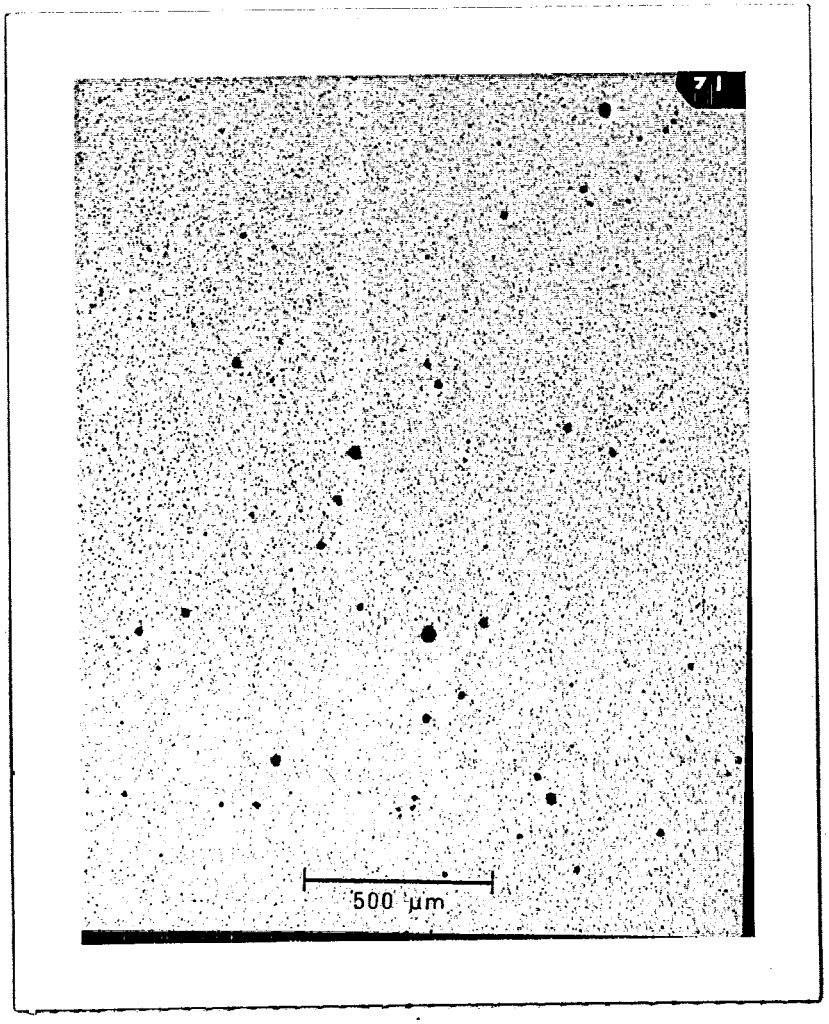

Figure 1.2.2: Photomicrograph of a 6111 deposit - low porosity - "wet" spray - small pores

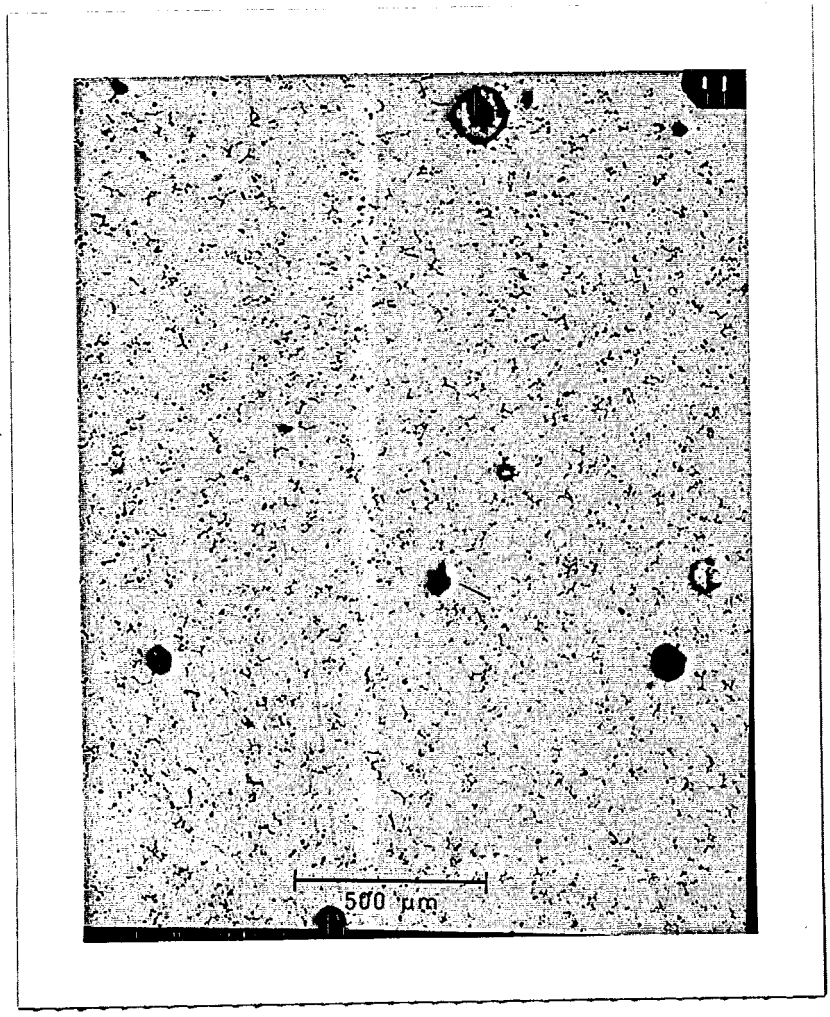

Figure 1.2.3: Photomicrograph of a 6111 deposit - low porosity - "wet" spray - large pores

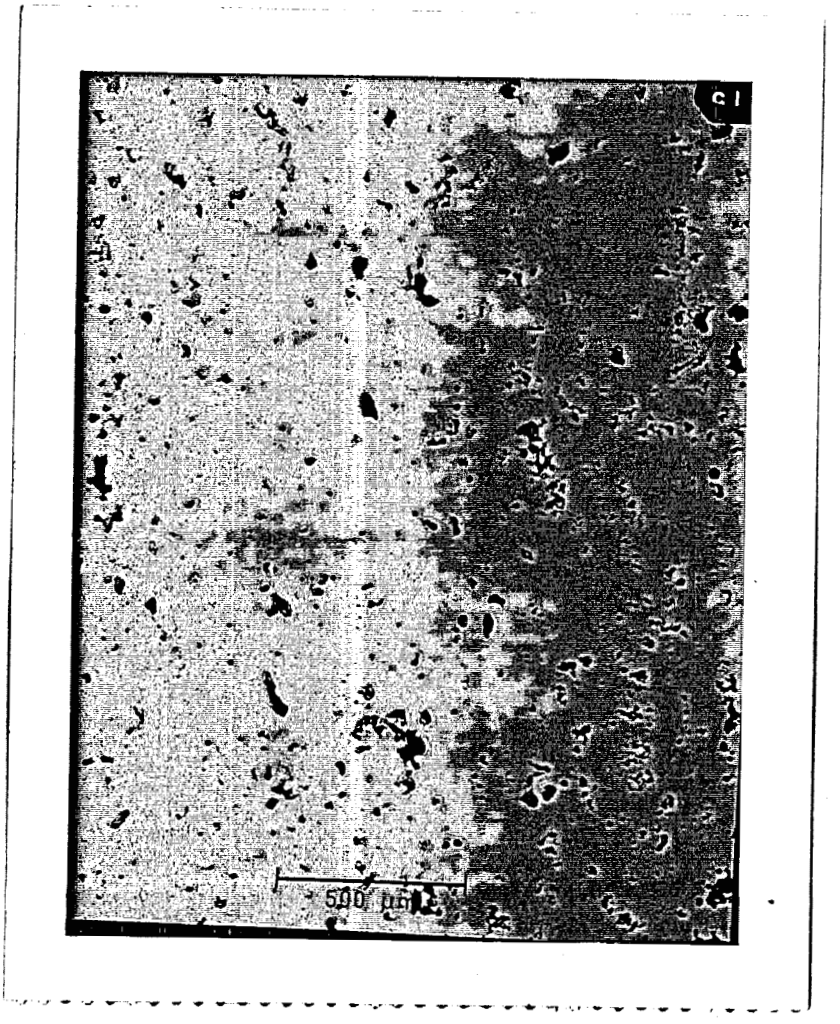

Figure 1.2.4: Photomicrograph of a 6111 deposit - high porosity - "wet" spray - large pores

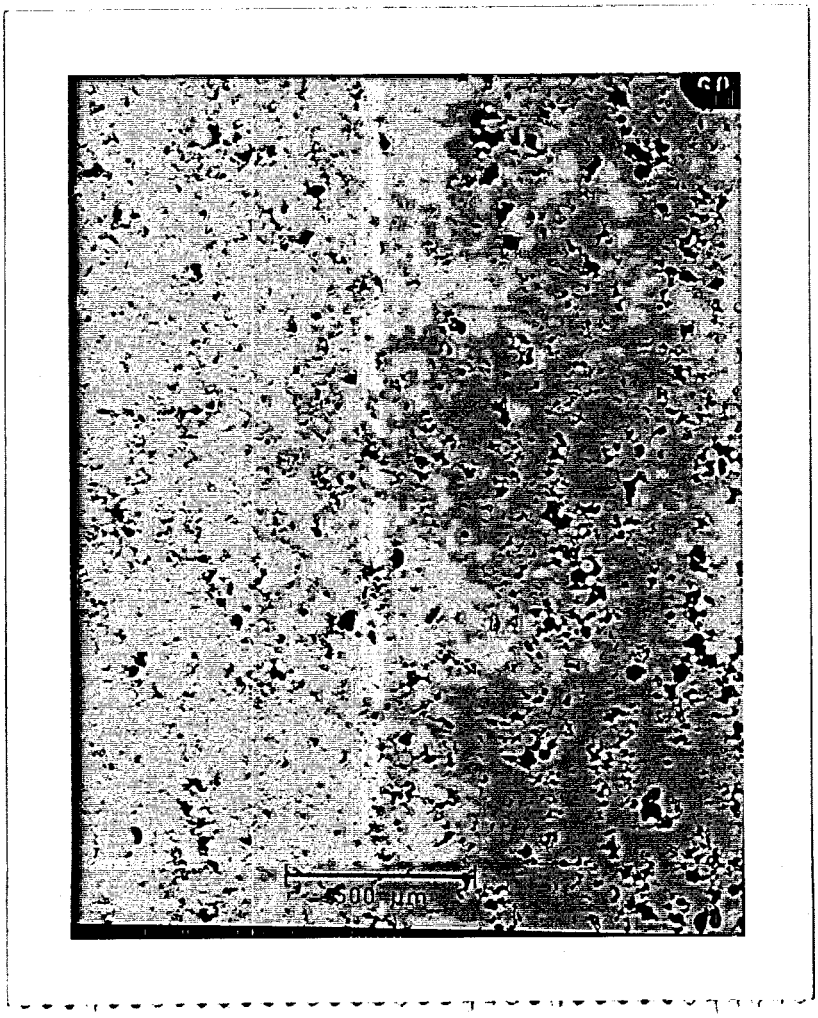

Figure 1.2.5: Photomicrograph of a 6111 deposit - high porosity - "dry" spray

8" A-3-b

NOZZLE: CENTER

0.04" GAS GAP

GAS FLOW 60.9 lb/min

Baffles None

Gauze S.S.

Protrusion 0.150

Set	Act	
52	52	1 S End
80	60	2 S. Mid
80	57	3 Cen
81	60	4 N. Mid
56	53	5 N. End

TEST 116 End

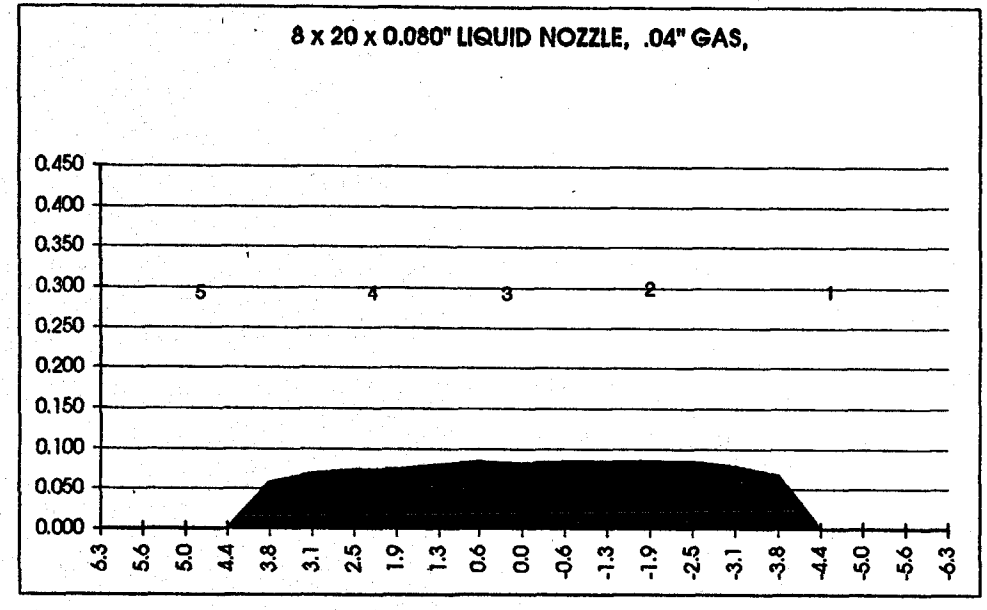

	Ht. In.	Tubes (In)	Normalized
		6.3	0.000
1	0.000	5.6	0.000
2	0.000	5.0	0.000
3	0.000	4.4	0.000
4	0.341	3.8	0.057
5	0.410	3.1	0.069
6	0.438	2.5	0.073
7	0.443	1.9	0.074
8	0.477	1.3	0.080
9	0.500	0.6	0.084
10	0.488	0.0	0.082
11	0.498	-0.6	0.083
12	0.501	-1.3	0.084
13	0.506	-1.9	0.085
14	0.502	-2.5	0.084
15	0.465	-3.1	0.078
16	0.399	-3.8	0.067
17	0.000	-4.4	0.000
18	0.000	-5.0	0.000
19	0.000	-5.6	0.000
		-6.3	0.000

3.1 TO -3.1" STAND. DEV. =	0.01438	0.0054
3.8 TO -3.8" STAND. DEV. =	0.03417	0.0085
Peak-to-Valley (-3.8 to 3.8)	0.1	0.02764745
Area Off Substrate. =		0.0000

Figure 1.2.6 "Best' measured deposit profile for 8" substrate

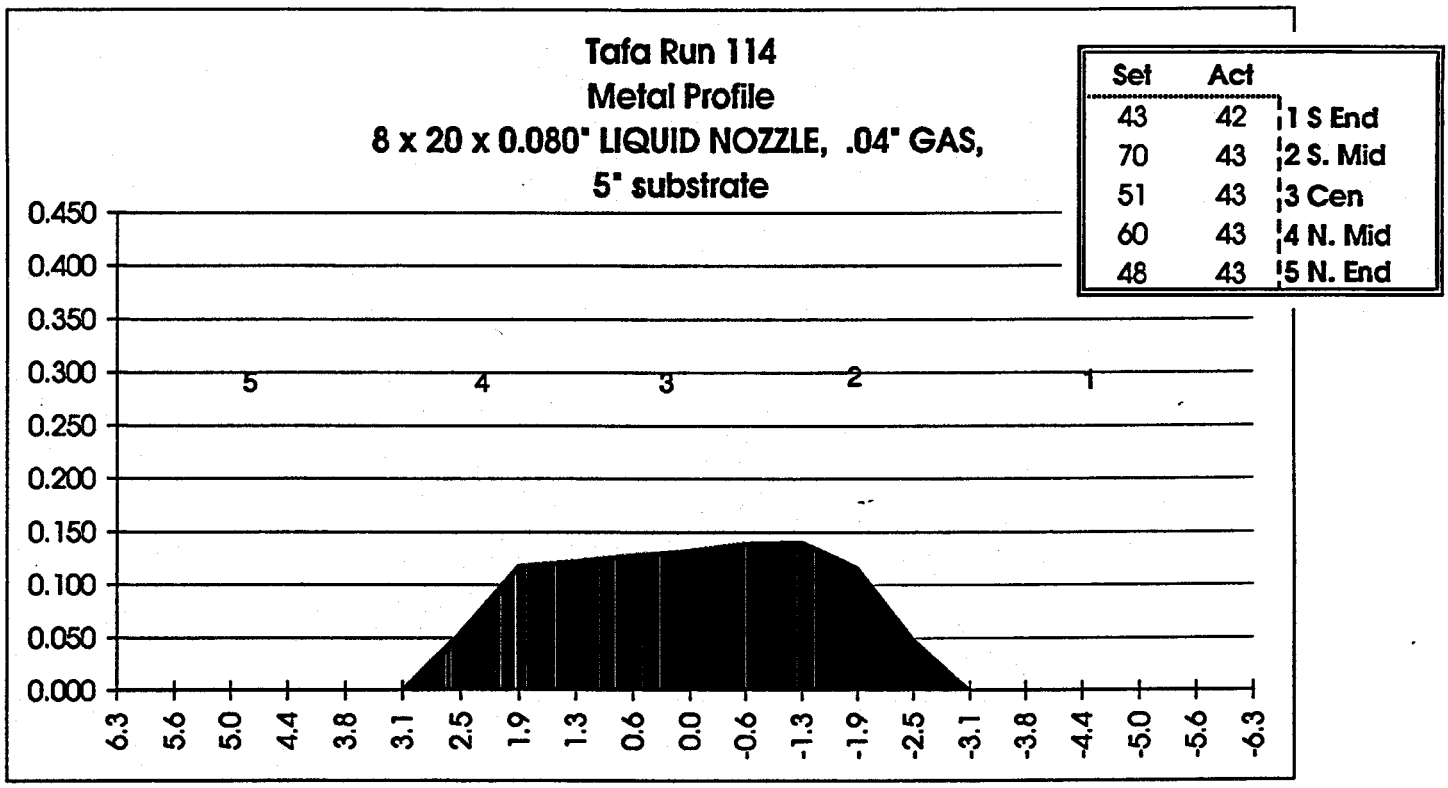

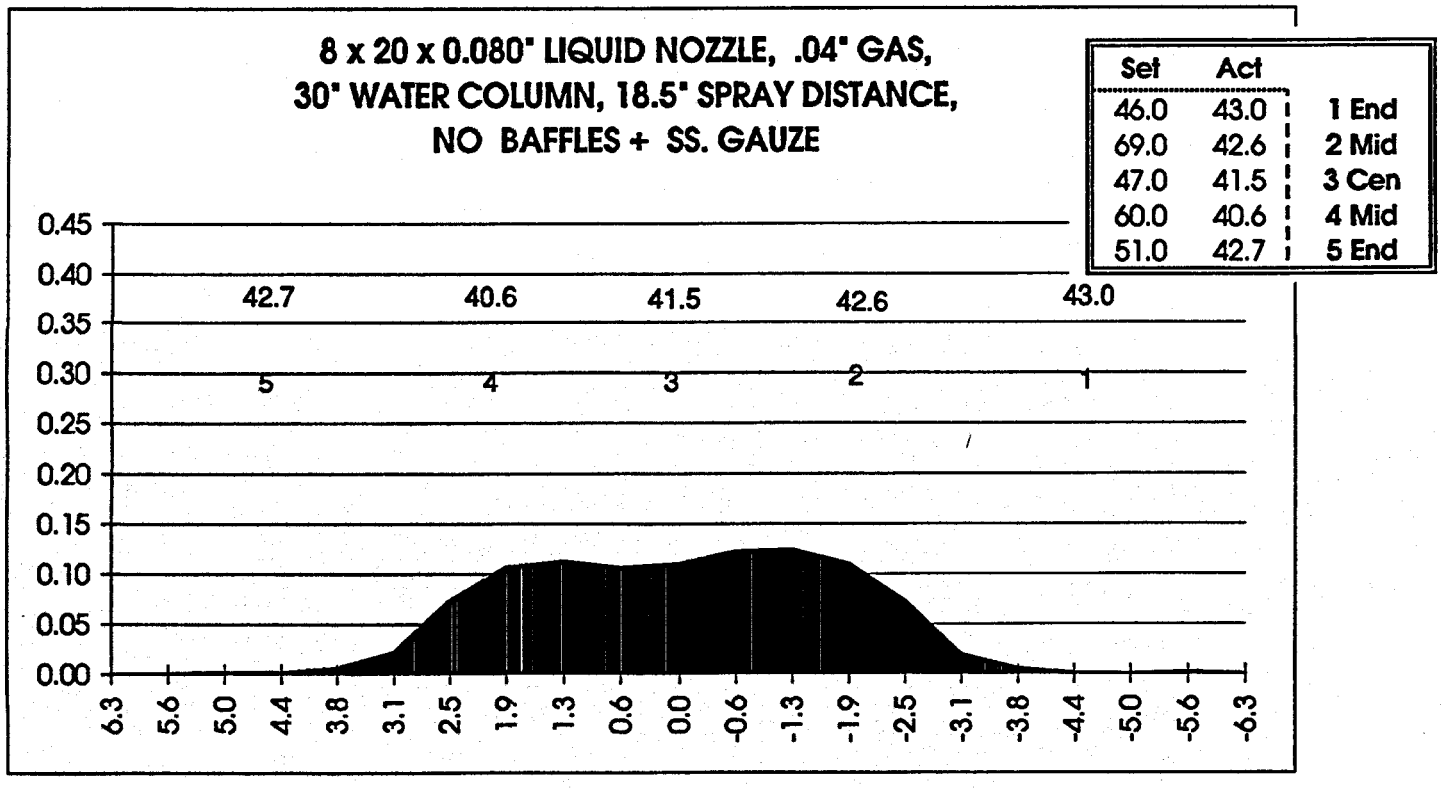

Figure 1.2.7 Comparison of metal and water spray profiles - 5" substrate

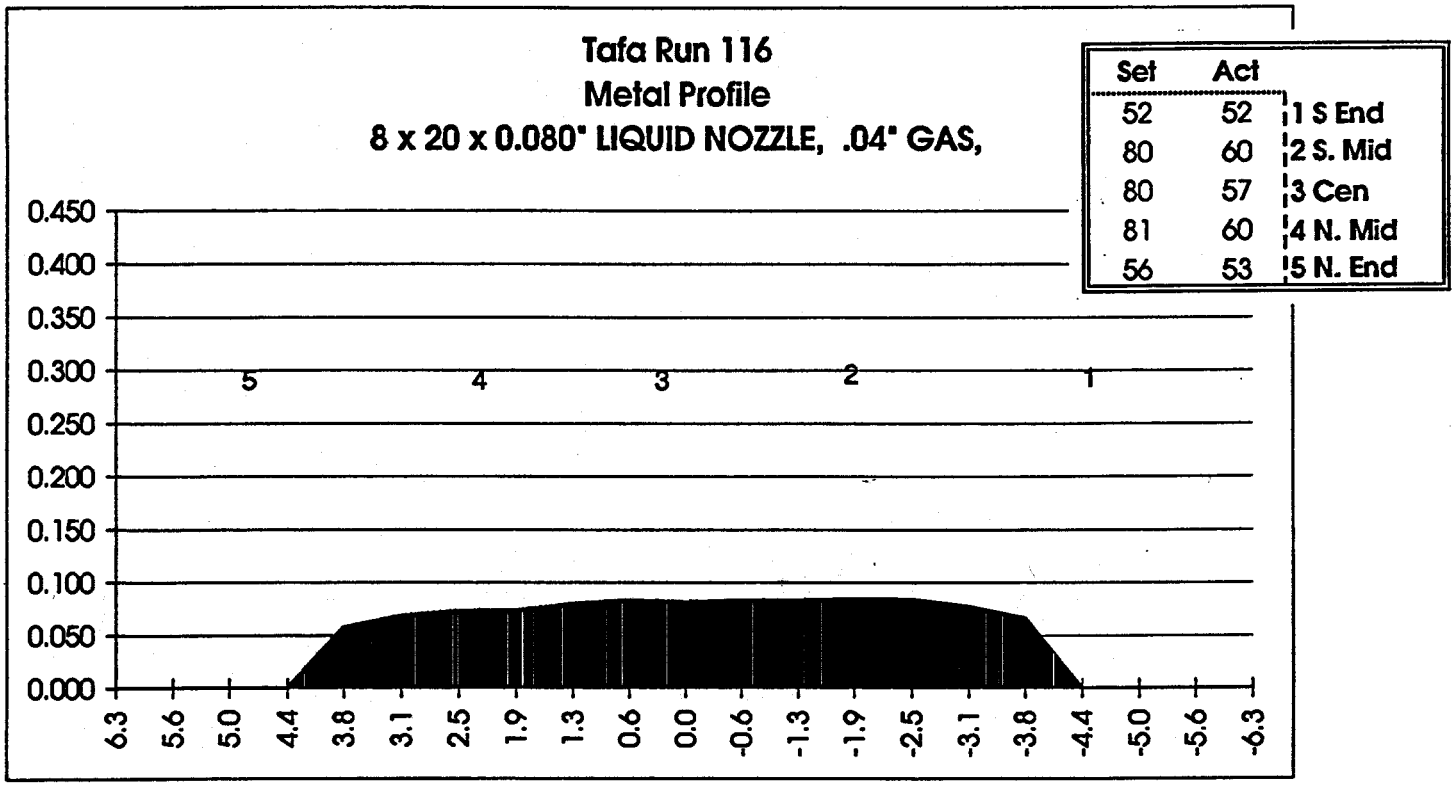

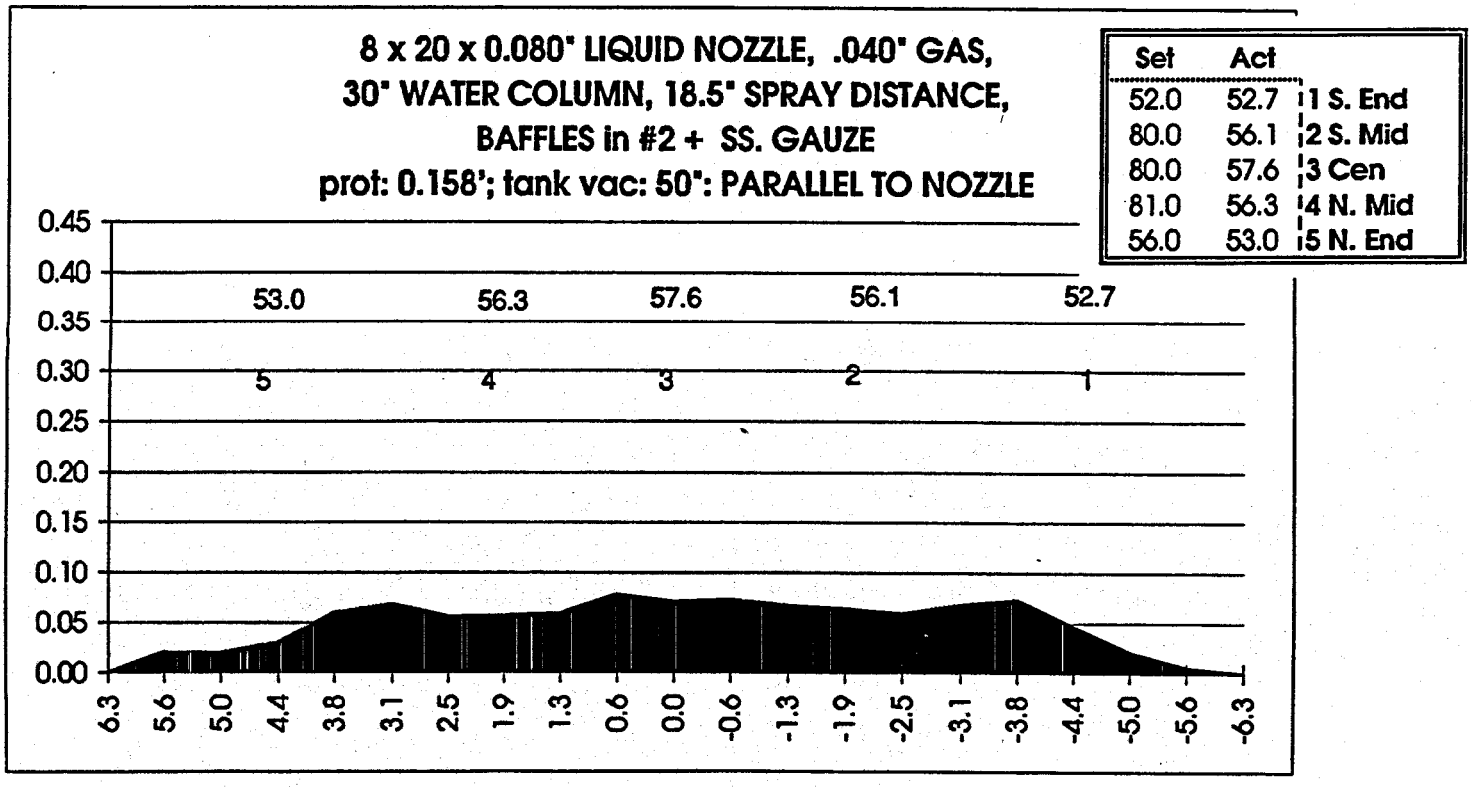

Figure 1.2.8 Comparison of metal and water spray profiles - 8" substrate

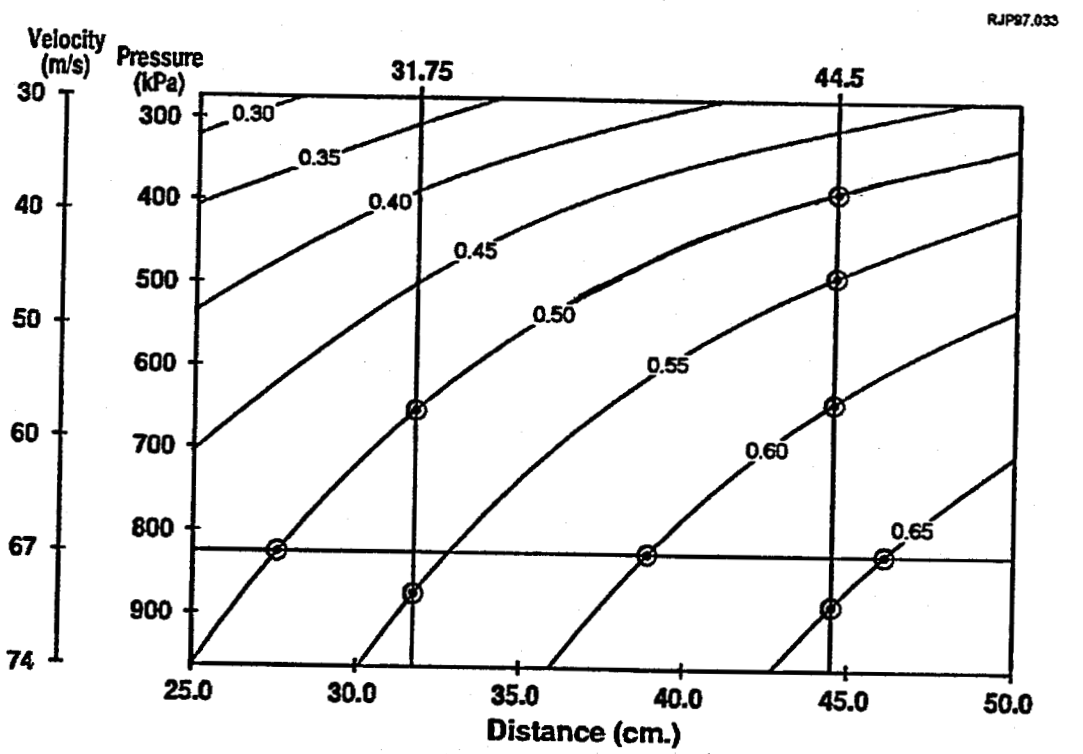

Figure 1.2.9 Test matrix based on spray model predictions for Marko spray chamber

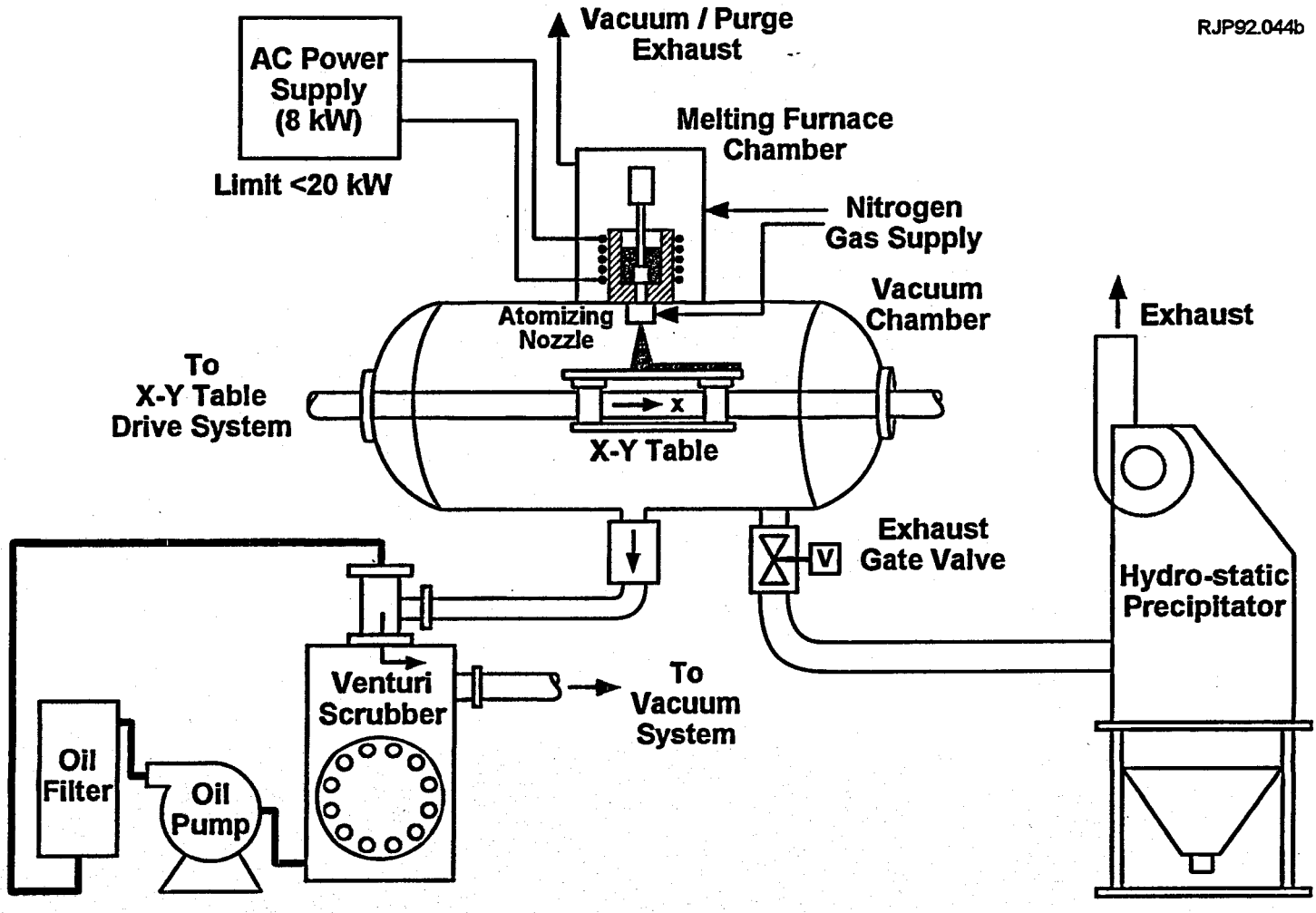

Figure 1.3.1: Tafa vessel schematic

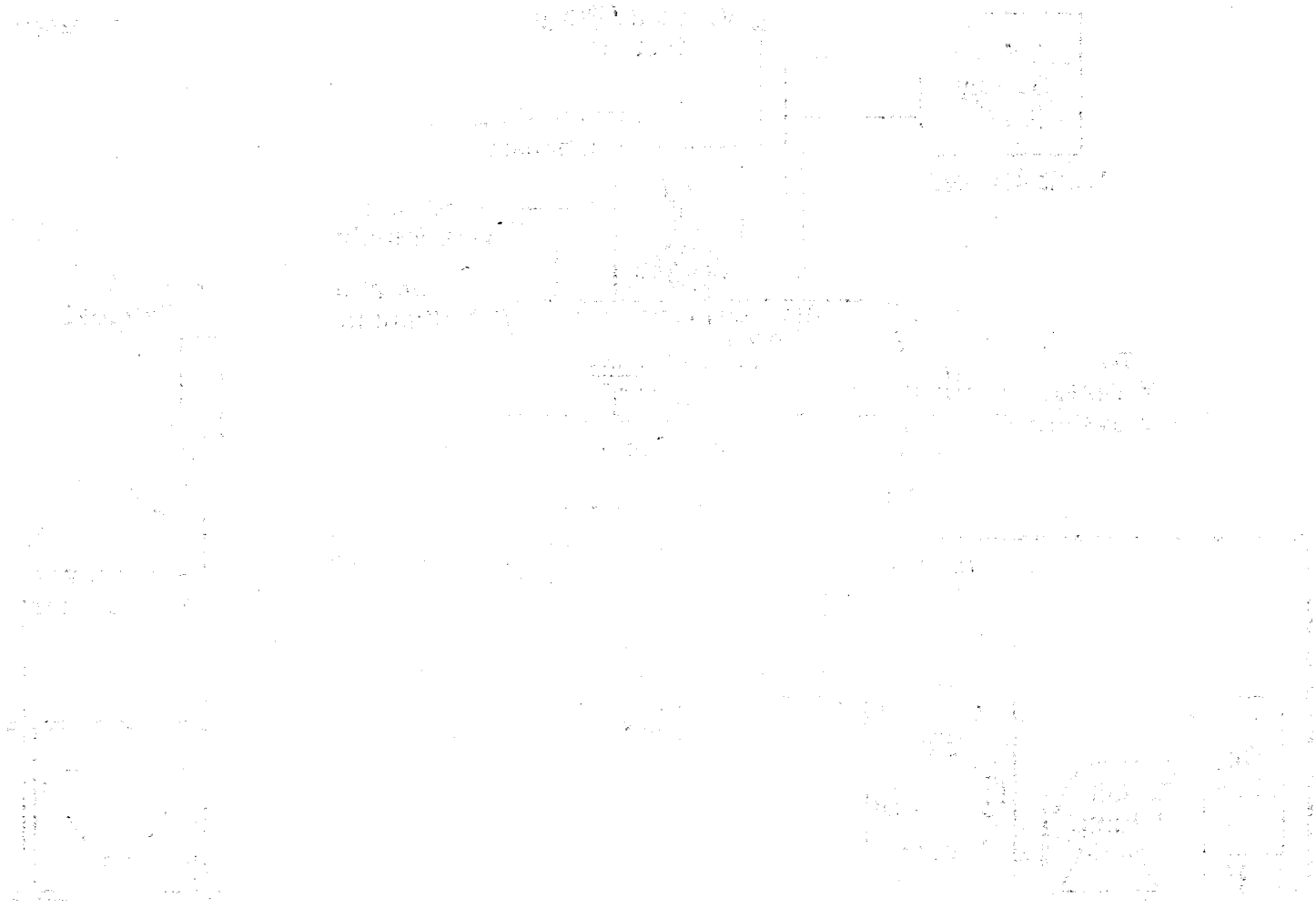

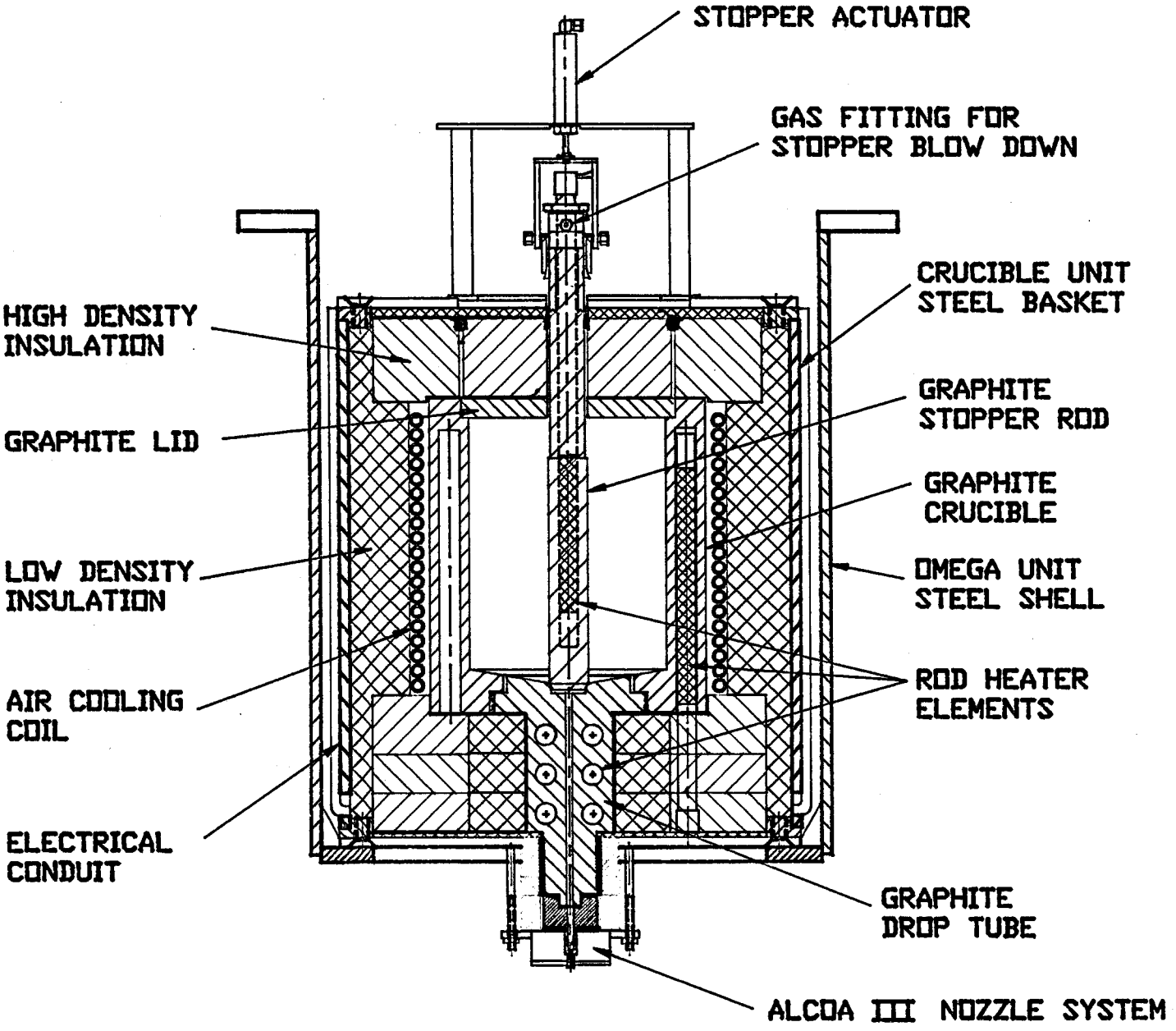

Figure 1.3.2: Melting furnace and nozzle basket assembly concept

Figure 1.4.1 Photograph of as-sprayed deposit **C**

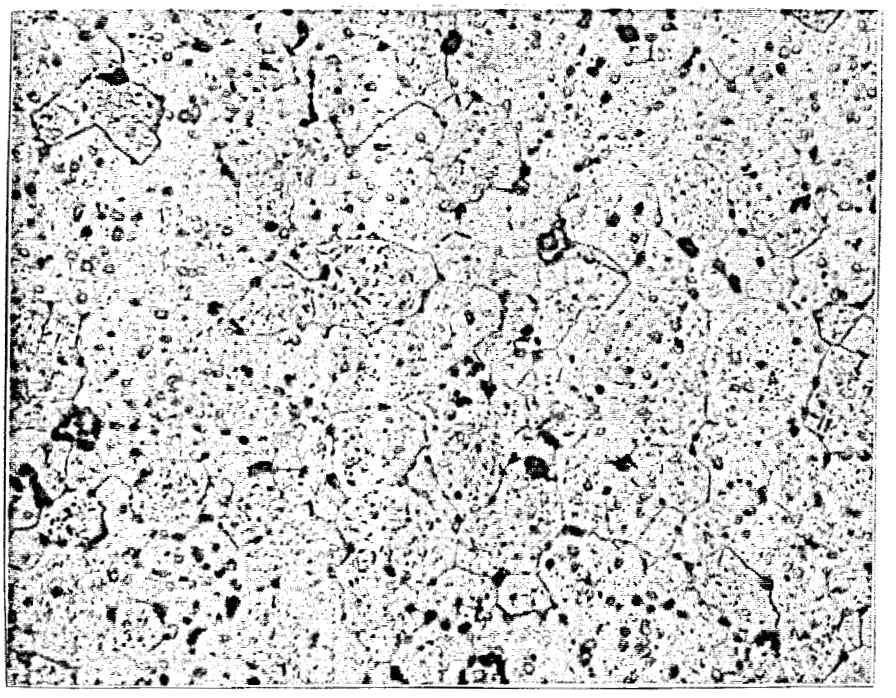

Figure 1.4.2 Photomicrograph of spray formed 6111 alloy - 200X

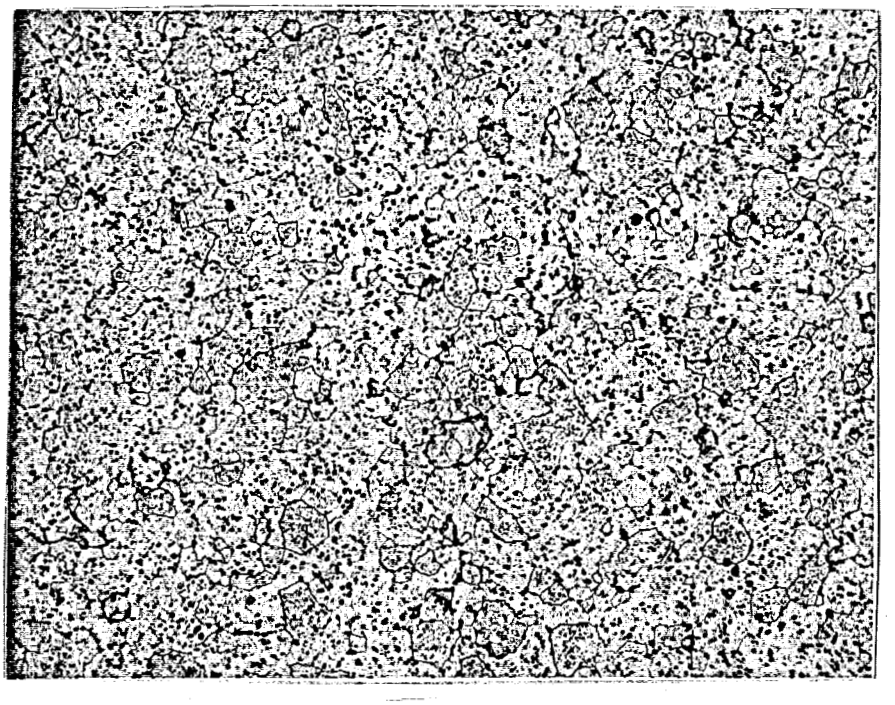

Figure 1.4.3 Photomicrograph of spray formed 6111 alloy - 50X

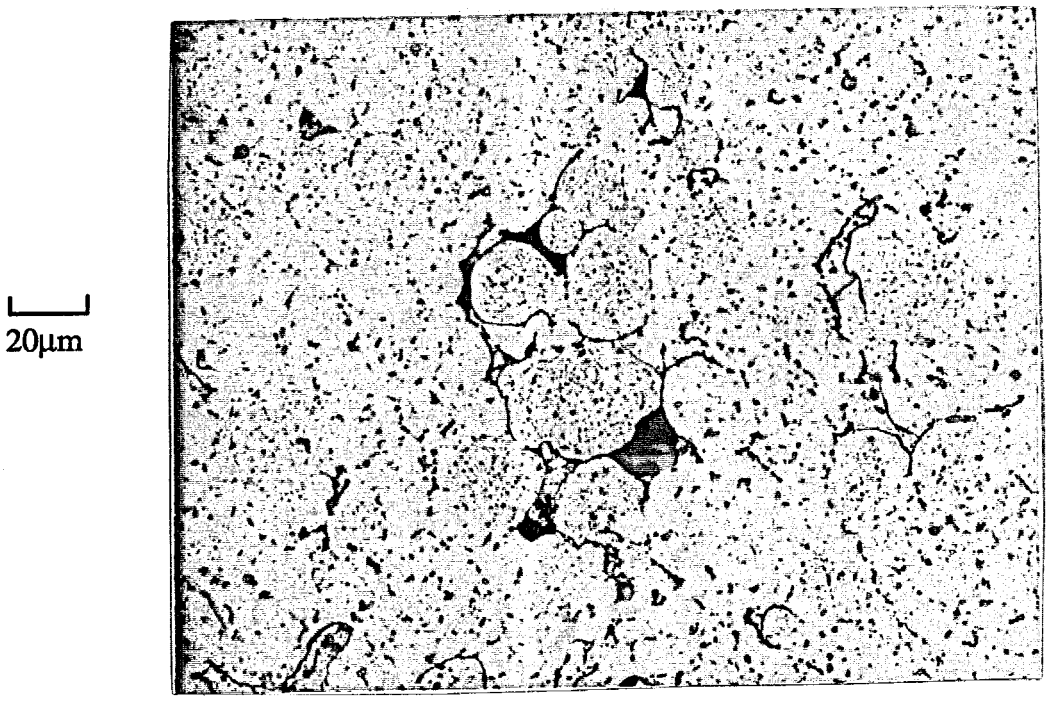

Figure 1.4.4 Photomicrograph of deposit C showing fine irregular porosity

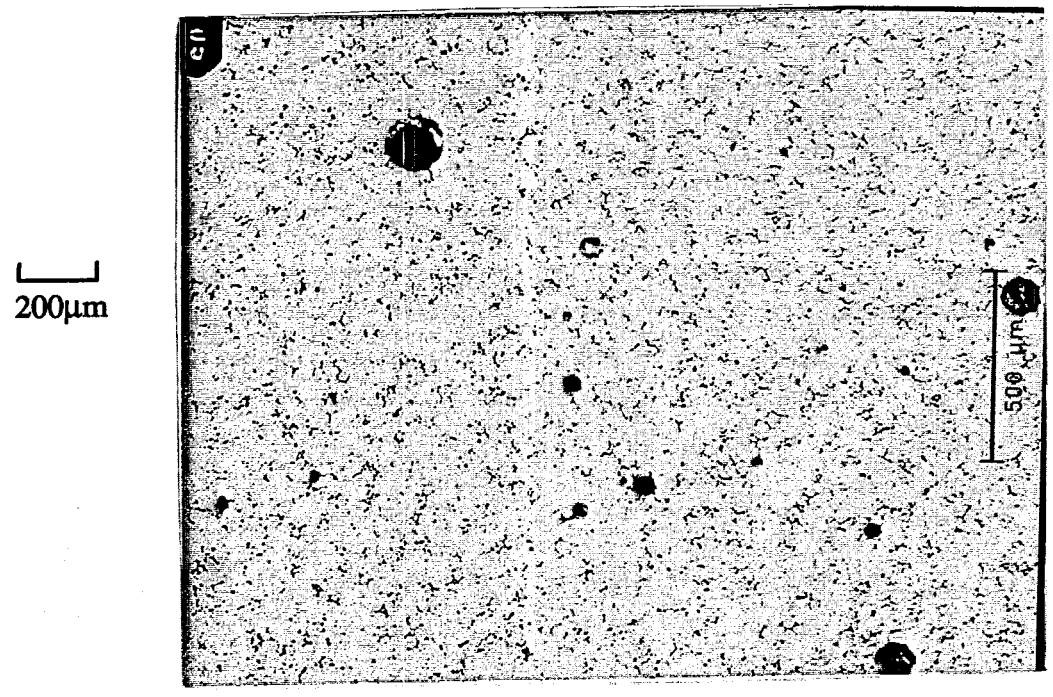

Figure 1.4.5 Photomicrograph of deposit A/B showing large rounded pores

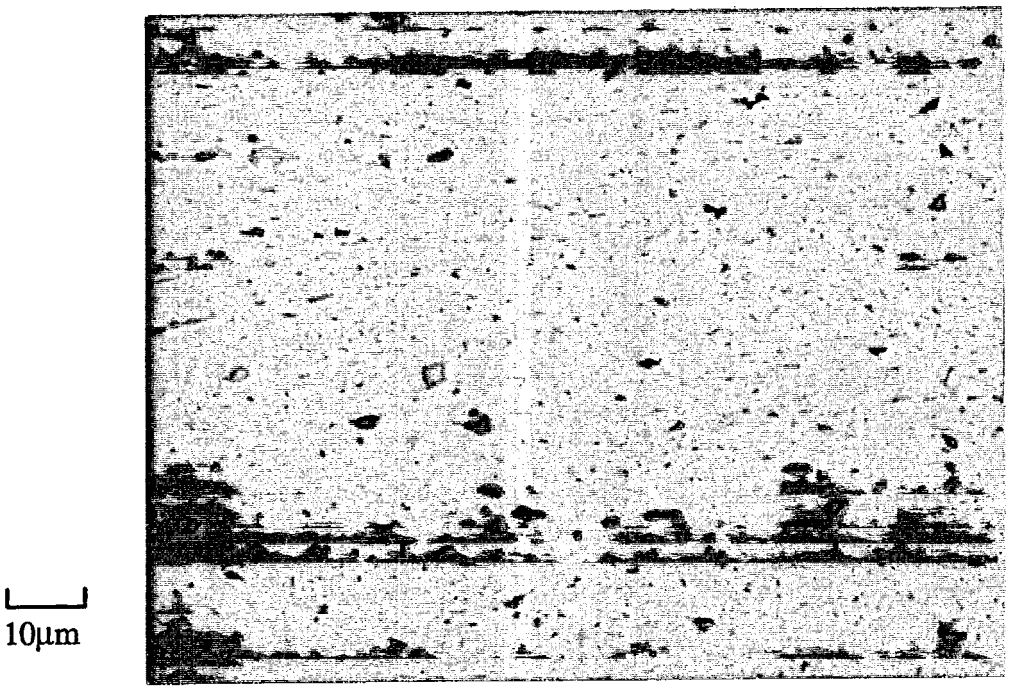

Hot Roll
Simulated Coil Cool
No Anneal

10μm

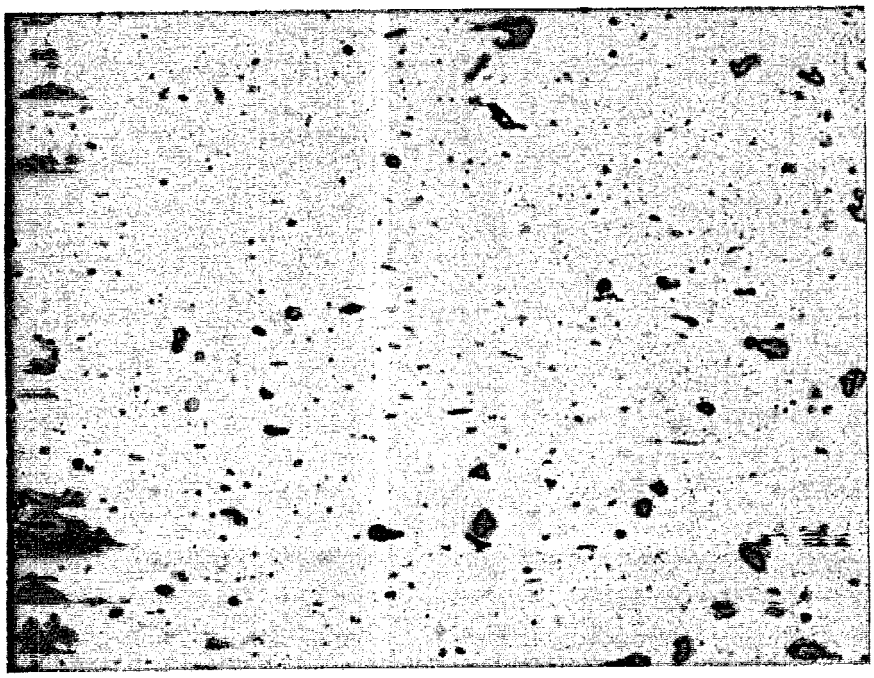

Hot Roll
Simulated Coil Cool
+ Anneal

ST
L

Etched with .5% Hf

Figure 1.4.6 Effect of intermediate gage anneal on second phase particles. Second phase particles appear to be coarser after the anneal. 6111 sheet after hot rolling and simulated coil cool.

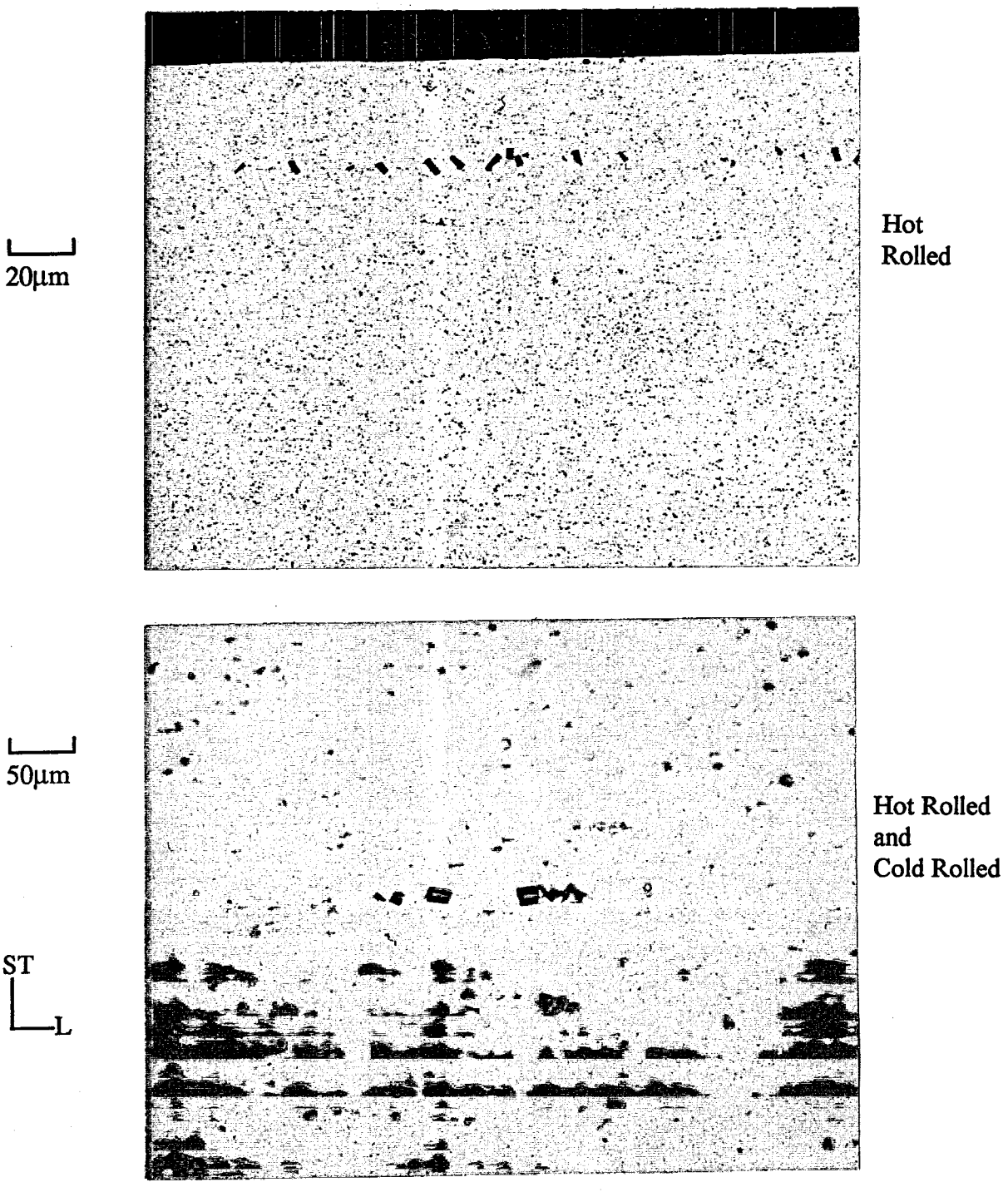

Figure 1.4.7 Spinnel (Al, Mg, Si, O_2) in 6111 sheet. These particles can be removed by standard molten metal filtration methods.

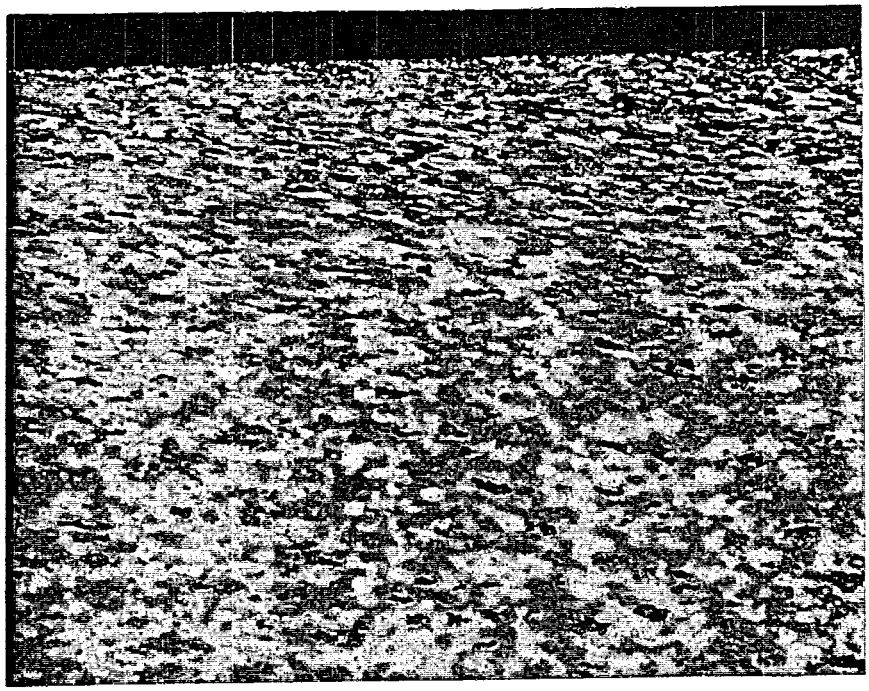

Hot Rolled
+
Simulated Coil Cool
and Gage Anneal

267μm

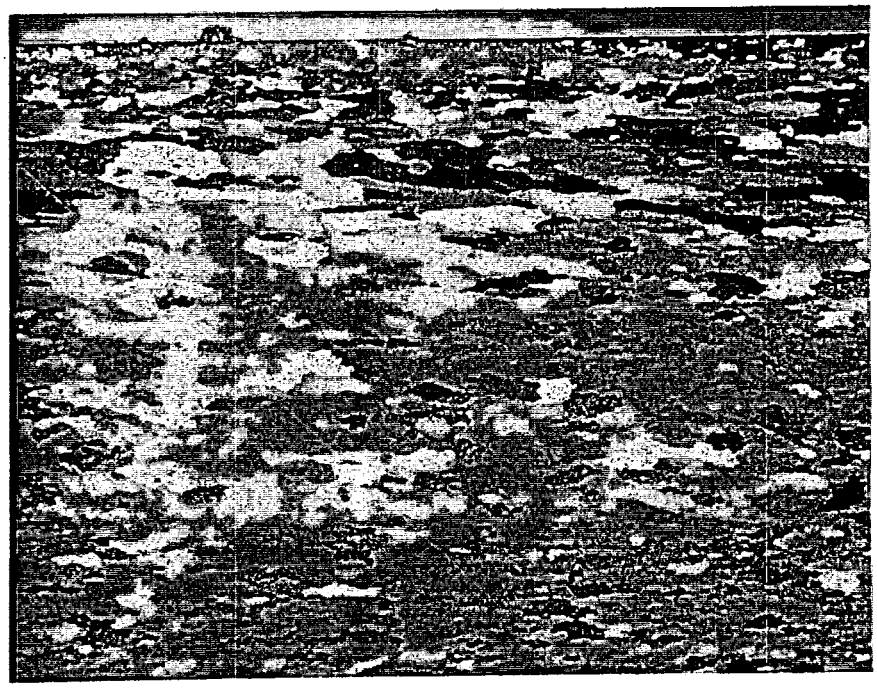

Hot Rolled
+
Simulated Coil Cool
and Gage Anneal

ST
L

Electro etched and photographed using polarized light.

Figure 1.4.8 Effect of hot work reduction and intermediate gage anneal on 6111 sheet. Both sheets appear to be fully recrystallized as a result of the anneal.

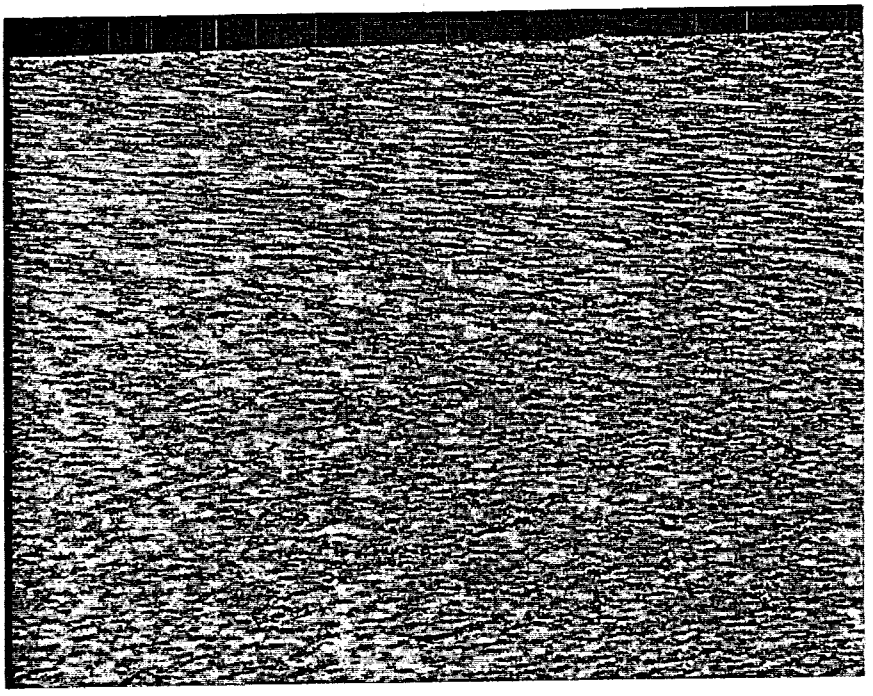

Hot Rolled
Simulated Coil Cool
No Anneal

267μm

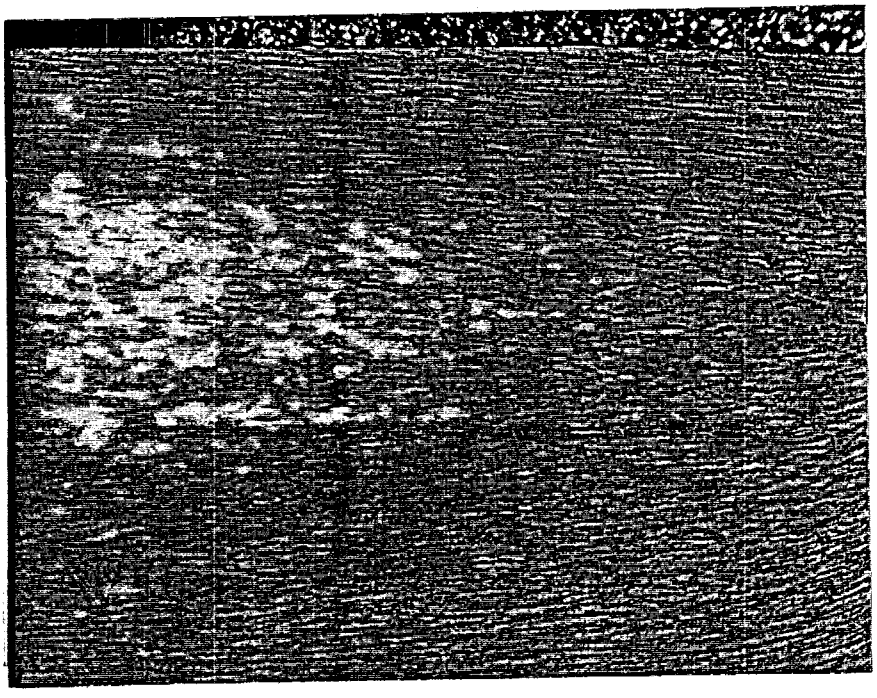

Hot Rolled
Simulated Coil Cool
No Anneal

ST
L

Electro etched and photographed using polarized light.

Figure 1.4.9 Effect of hot work reduction on 6111 sheet.

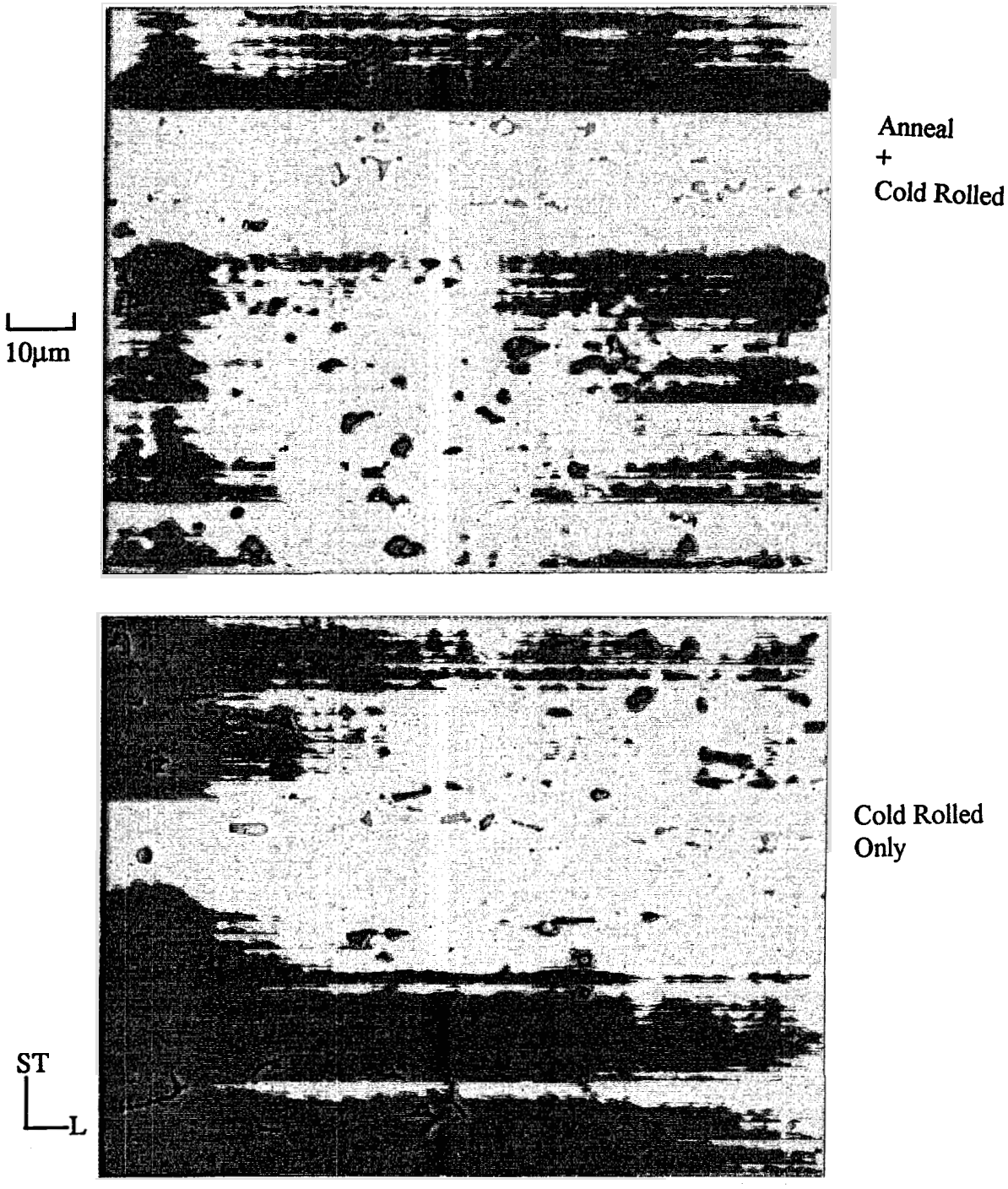

Figure 1.4.10 Solution heat treated 6111 cold rolled sheet.

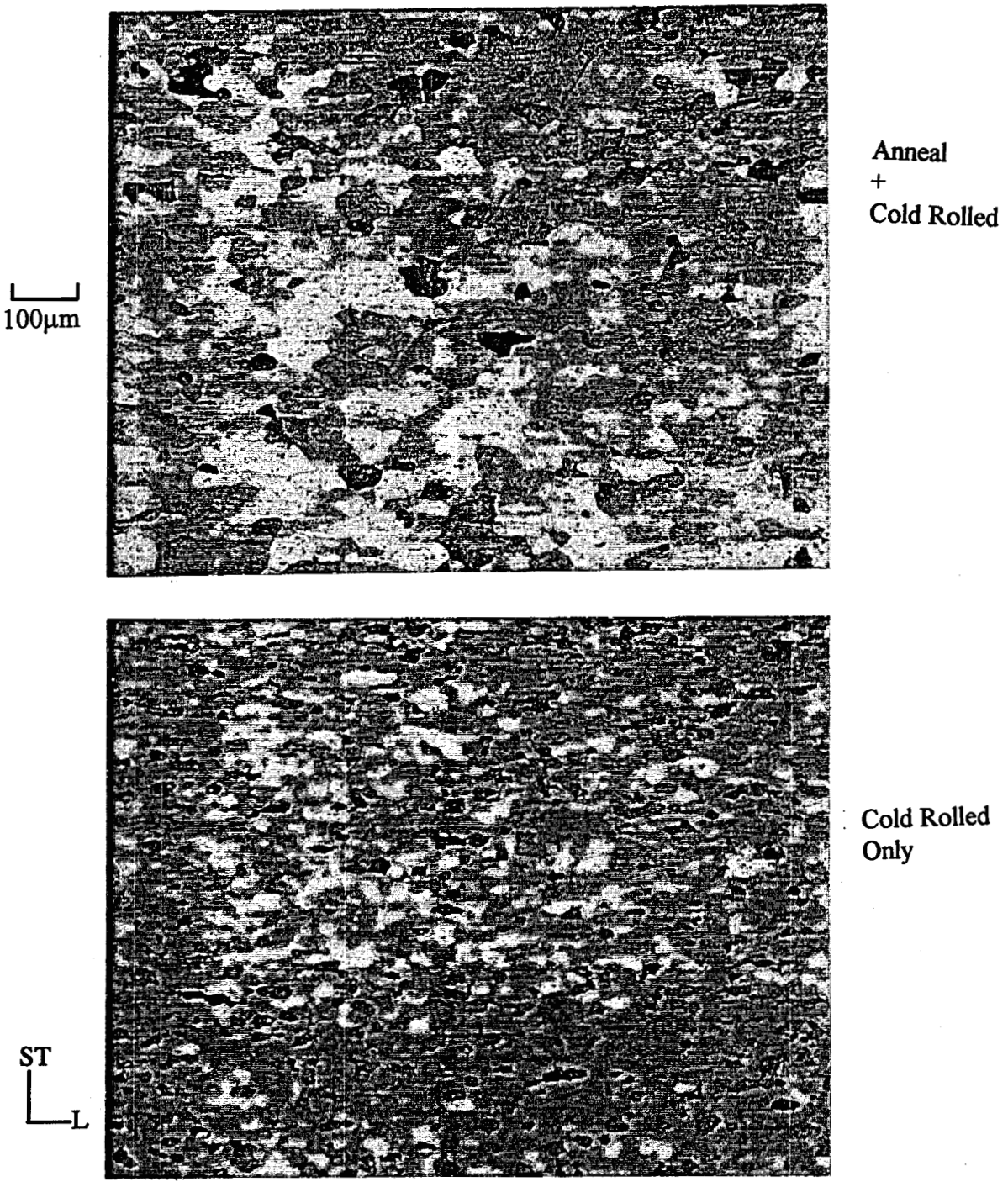

Figure 1.4.11 Grain structure in cold rolled and solution heat treated 6111 sheet.

Figure 1.5.1: Predicted three dimensional profile of deposit on flat substrate in a large rectangular chamber in shaded form

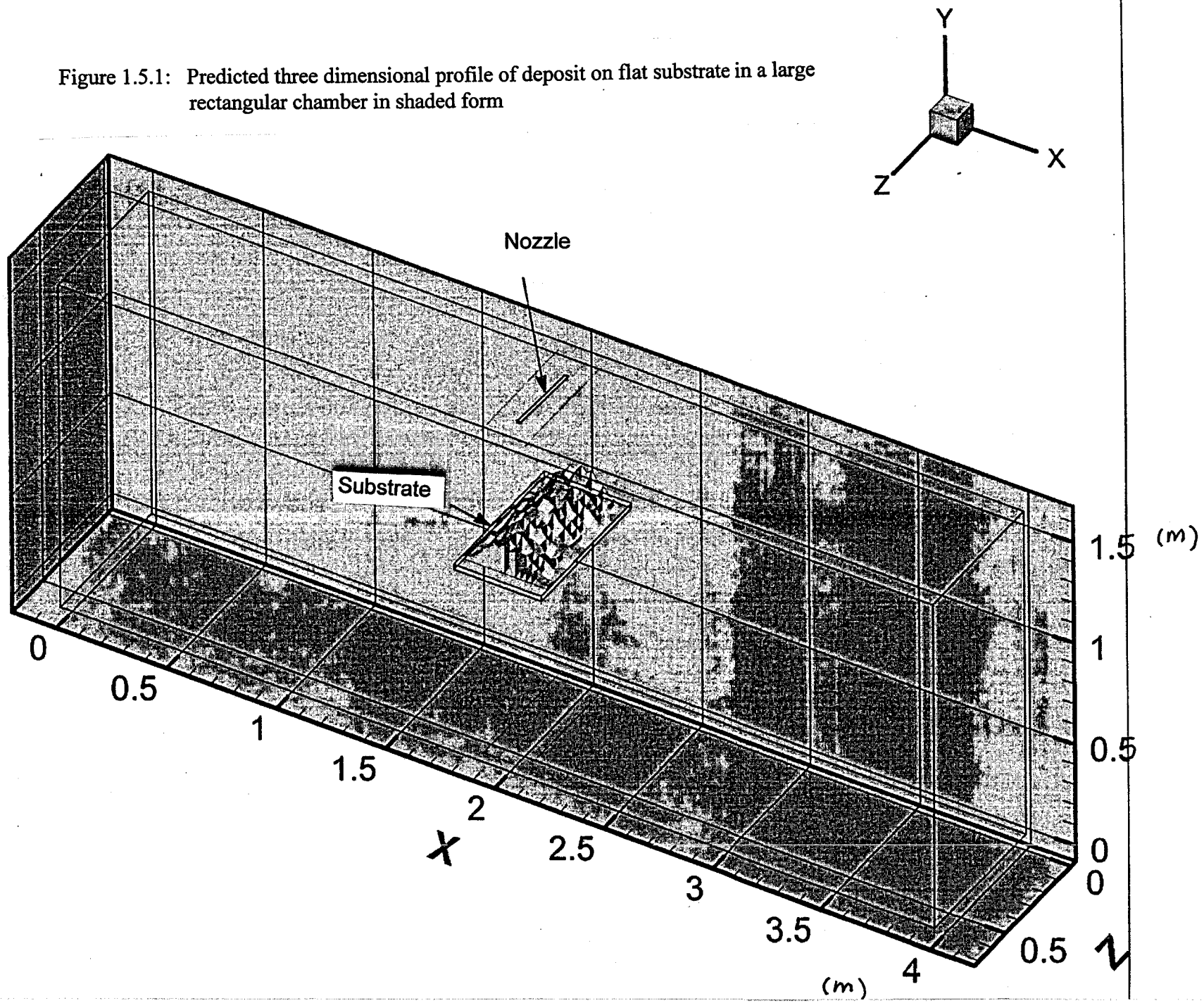

Figure 1.5.2: Predicted three dimensional profile of deposit on flat substrate in a large rectangular chamber in surface perimeter form

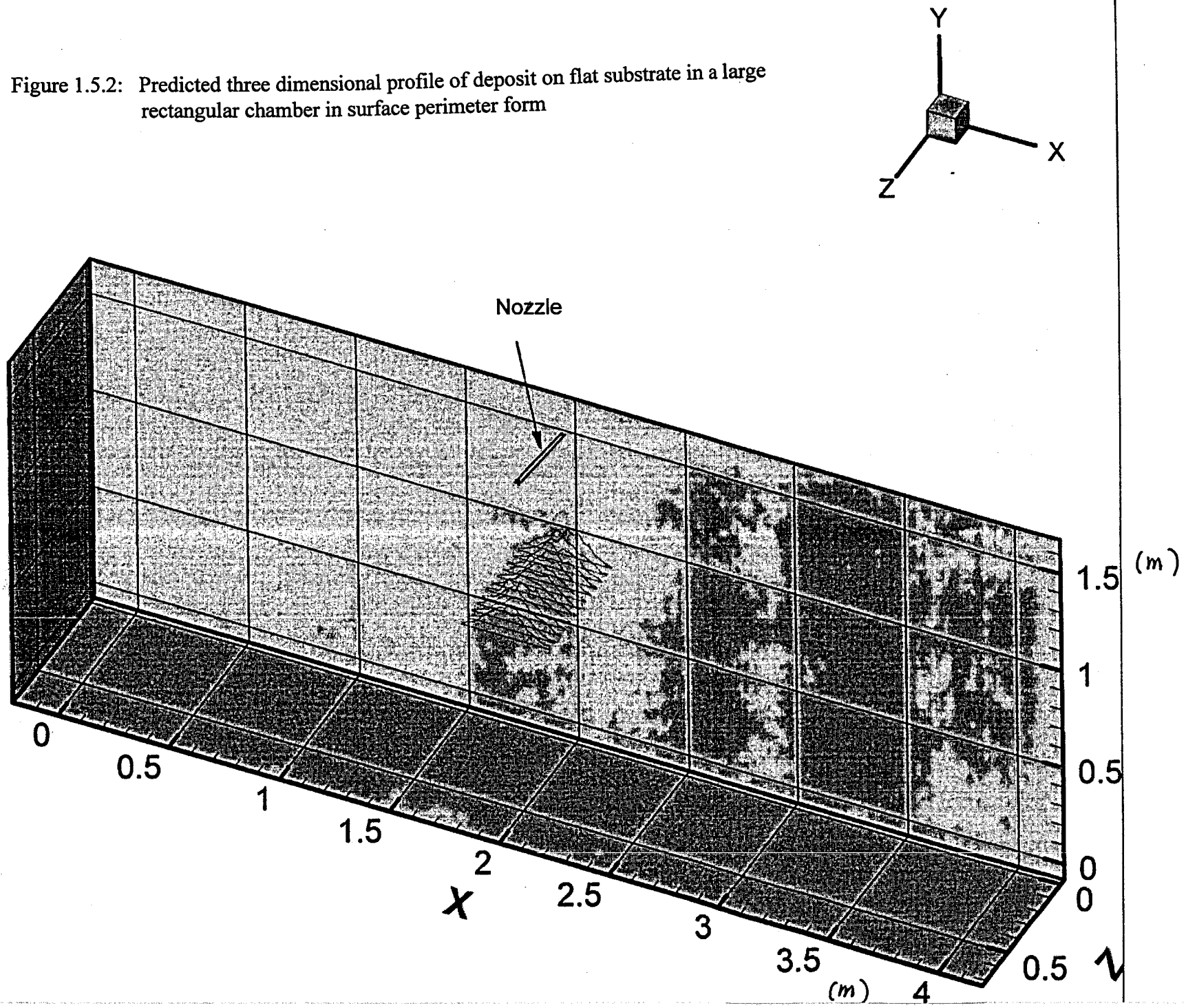

Figure 1.5.3: Predicted three dimensional profile of deposit on flat substrate in a smaller rectangular chamber in surface perimeter form

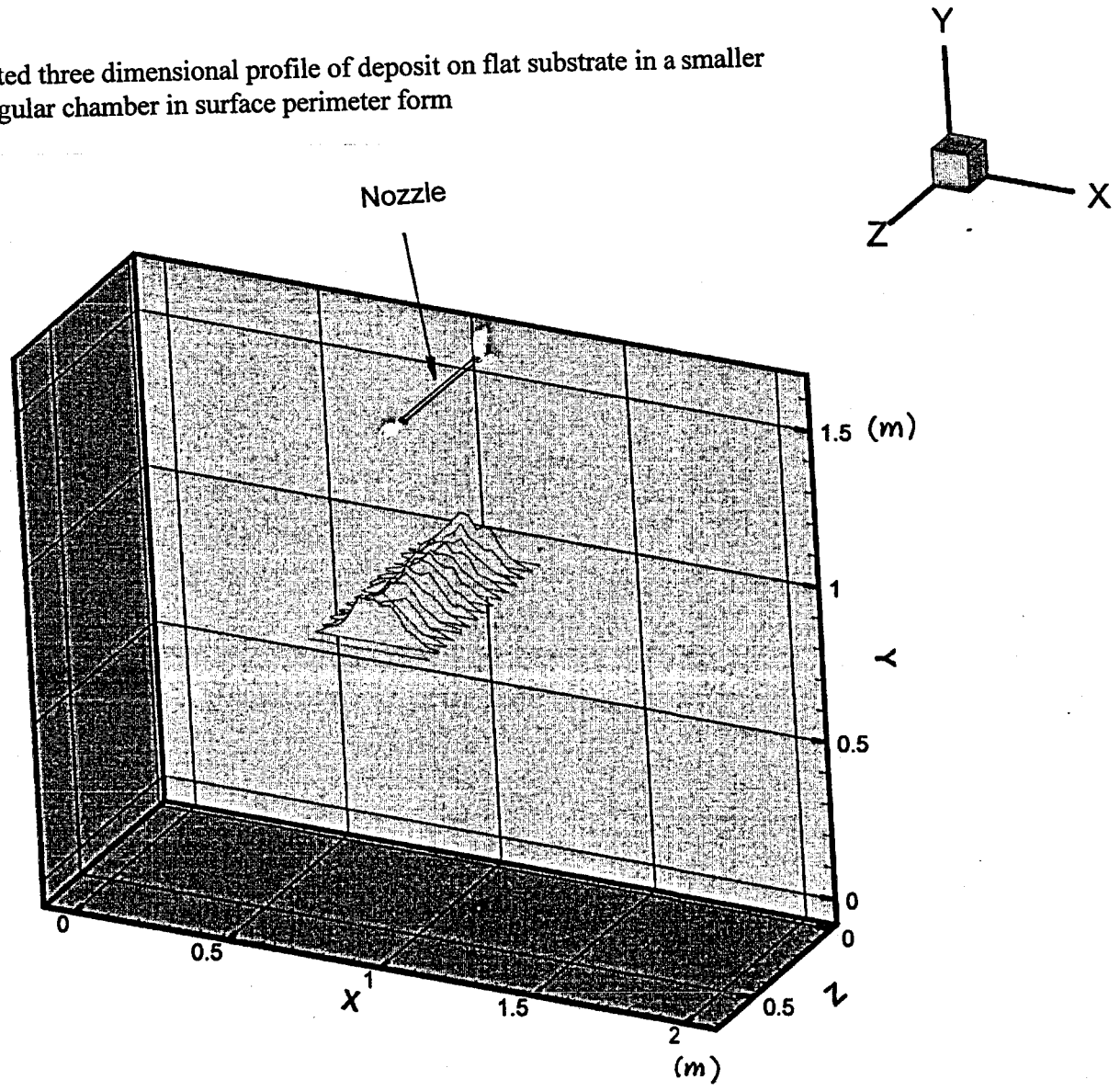

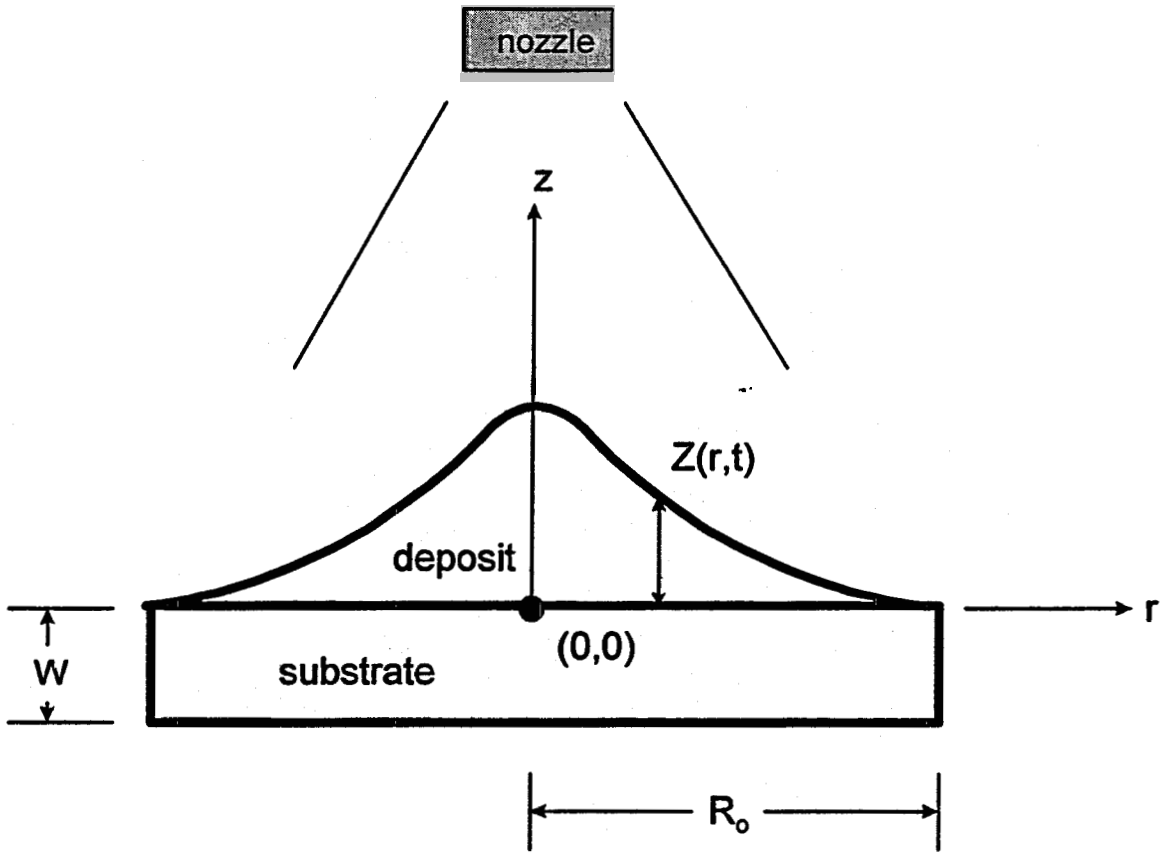

Figure 1.5.4: Schematic drawing of the deposit and substrate system for modeling

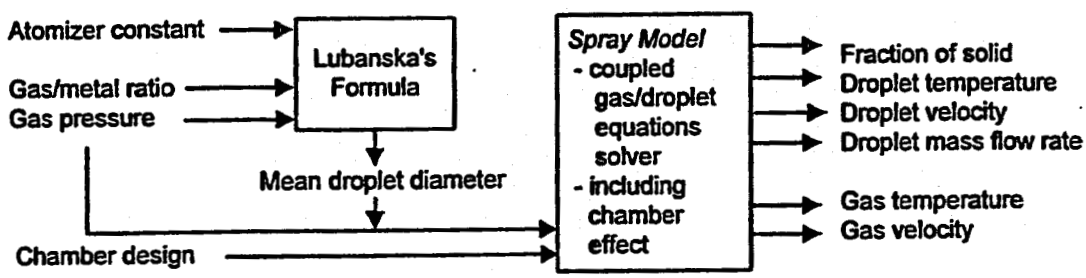

Figure 1.5.5 Input and output of the spray model

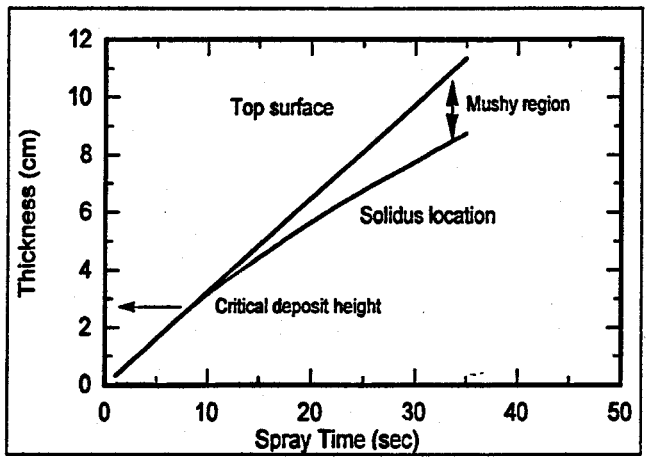

Figure 1.5.6. Location of the Top Surface and Solidus Isotherm vs. Spray Time (Solid Fraction = 0.6).

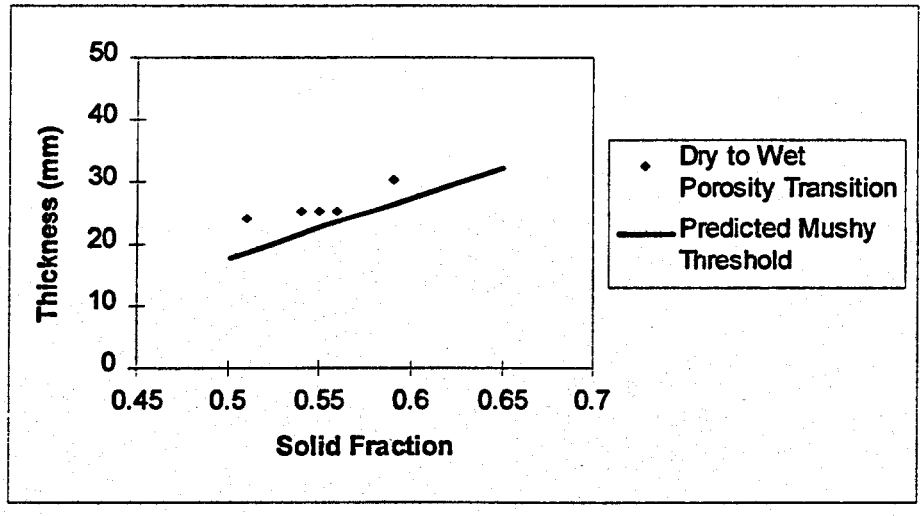

Figure 1.5.7 Predicted Mushy Threshold and Porosity Transition vs. Solid Fraction.

APPENDIX I

AN APPROACH TO MINIMIZE POROSITY IN SPRAY FORMED DEPOSITS THROUGH A MODEL-BASED DESIGNED EXPERIMENT

Robert L. Kozarek
M. G. Chu
S. J. Pien
Alcoa Technical Center
100 Technical Drive
Alcoa Center, PA 15069-0001, USA

Abstract

This paper describes a designed experiment to develop a process map of spray conditions in relation to porosity in the bulk deposit. The experiments were performed on a small bench scale unit. The process conditions were selected on the prediction of solid fraction of droplets using a mathematical model of the spray process. Process parameters considered include gas pressure, gas/metal ratio, spray distance, average droplet velocity, average droplet diameter and melt superheat. An operating window for minimizing porosity in the bulk was identified using a transient model to describe the thermal history and fraction solid at each location in the small scale deposit. The application of this modeling methodology to determine the optimum processing parameters in a larger scale unit is described.

1. Introduction

Spray forming technology is based on the atomization of liquid metals and subsequent deposition on a substrate. In the process, gas atomized metal droplets are simultaneously cooled as they are conveyed to the substrate by the atomizing gas. The extent of cooling is dependent on the characteristics of the spray such as particle and gas velocity, the particle size, and the time of flight. Depending on the thermal history, the impacting droplets will arrive at the substrate in either a fully solid, fully liquid or mushy state. Under the proper conditions, the mixture of droplets will consolidate to form a thin mushy or semi-solid deposit on the top surface of the spray formed deposit. This layer solidifies incrementally as heat is transferred into the substrate. Some porosity is nearly always present in the solidified deposits. The thickness and average solid fraction of the mushy layer are important dependent parameters which have been strongly correlated to the porosity and product microstructure of the deposit. Unfortunately, neither quantity can be experimentally measured directly. They must be inferred by some other method.

For commercial application of spray forming technology, it is necessary to eliminate undesirable porosity. One approach is to "heal" porosity by means of thermomechanical processing such as rolling, extrusion, forging, etc. to achieve full density and properties. Another is to optimize the spray forming process parameters to minimize the porosity level in the deposit. Ultimately, a combination of the two approaches is likely to be needed.

The nature of porosity varies with the type of deposit and processing conditions. For sheet products in which a deposit is produced by spraying onto a moving substrate to a desired thickness, two types of porosity are observed. Near the substrate is a very porous region in which the pores are irregular and interconnected. For aluminum alloys, pores can be as large as 2000 μm in size. This "base porosity" can extend up to 0.6 cm in thickness depending on the spray conditions in the leading edge of the spray and the temperature, thickness and properties of the substrate. Further from the substrate in the bulk deposit region, the pores become isolated and equiaxed or spherical in shape ranging in size from 20 to 150 μm. The large pores tend to be spherical and the smaller pores tend to be equiaxed. The size and distribution of the pores are strongly dependent on the spray conditions. The mechanism for "base" porosity and "bulk" porosity formation are different and will require different process modifications to minimize each type of porosity.

In this investigation, we performed a designed experiment to optimize processing conditions to minimize "bulk porosity." Mathematical models were used both to design the experiments and analyze the results. To examine the effects of atomizing gas pressure, gas/metal ratio, spray distance, average droplet velocity, average droplet diameter and melt superheat, a semi-empirical steady state model of the process was used to predict the resulting fraction solid in the spray. Combinations of process conditions which yield a predicted fraction solid were selected for the test matrix in the designed experiment. Deposits were produced in a small scale spray forming unit using a stationary nozzle. The deposits were analyzed for porosity at fixed increments through the center section of the deposit. Because of the transient nature of the spray tests, process conditions were constantly changing as the deposits grow thicker. A second transient model was used to predict the solidification conditions and thermal history of the deposit at the sample locations of the deposit and the results were correlated with the porosity measurements.

2. Description of Steady State Spray Model

A numerical simulation model was developed to simulate the gas flow characteristics and droplet deposition in a spray forming chamber. This numerical model of the spray was used to predict the solid fraction of the atomized droplets arriving at the substrate surface. The model also predicts the velocity and thermal history of both the droplets and the gas in the spray and includes solidification modeling. Effects of pressure on droplet size distribution for the nozzle used in this study are estimated via a Lubanska [1] type correlation. Figure 1 shows a block diagram of the inputs and outputs of the spray model.

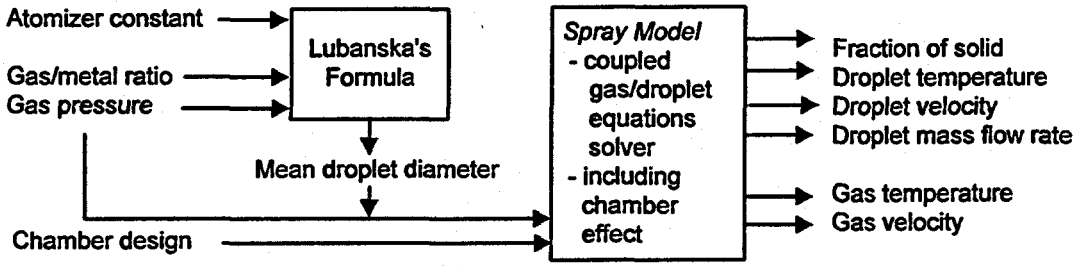

Figure 1. Inputs and Outputs of the Spray Model

In the spray model, Lagrangian forms of droplet momentum and energy equations are solved together with two-phase turbulent flow solutions. The coupled, transport equations of both dispersed droplets and continuous gas flow are solved simultaneously. For the gas phase, an Eulerian-Lagrangian approach is formulated treating droplets as discrete entities in a continuous gas field described with an Eulerian framework. The advantage of this droplet tracking approach is the capability of solving transport phenomena on the scale of droplet size. The governing equations as well as the basis of the physical models implemented in the numerical model is described by Chyu, et al. [2] and Ding, et al. [3].

3. Description of Transient Deposition Model

A transient model of the deposit and substrate is also developed and is used to predict the thermal history, thickness of the semi-solid layer, location of the top metal surface and location of the solidus temperature isotherm. In the deposition model, the first principle equations for the mass and energy transfers were formulated and solved numerically. Figure 2 shows schematically the system to be modeled. Both deposit and substrate are included in the analysis. Heat exchange by convection and radiation with the surroundings is described by using the effective heat transfer coefficients. At the interface, between the deposit and the substrate, an interfacial heat transfer coefficient is also assigned to include the interface resistance effect. At the upper surface of the deposit, however, energy is added to the layer by the hot droplets arriving at the substrate. The energy content and average mass flux of the arriving droplets are parameters which may be specified or determined on the basis of processing conditions by the aforementioned spray model. Details of the deposition model and solution procedures are described by Pien [3] for a linearly shaped deposition process. A similar work has been reported by Fritching [4] for cylindrically shaped deposits.

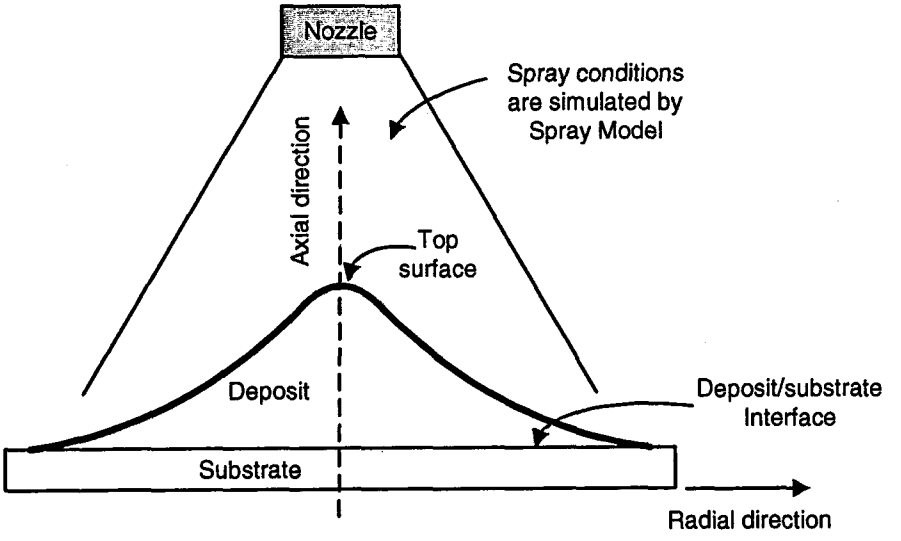

Figure 2. Schematic of Main Elements in Deposition Model

4. Experimental Setup

Spray formed deposits were produced using a small spray forming unit at the Alcoa Technical Center. A photograph and schematic of the unit is shown in Figure 3. The unit was equipped with an axisymmetric nozzle and an induction heated crucible. All deposits were produced using nitrogen gas and a proprietary aluminum alloy of fixed composition heated to a constant melt temperature. The substrate was 1.27 cm (½") mild steel plate. The flight distance was manually set by adjusting the vertical location of the substrate.

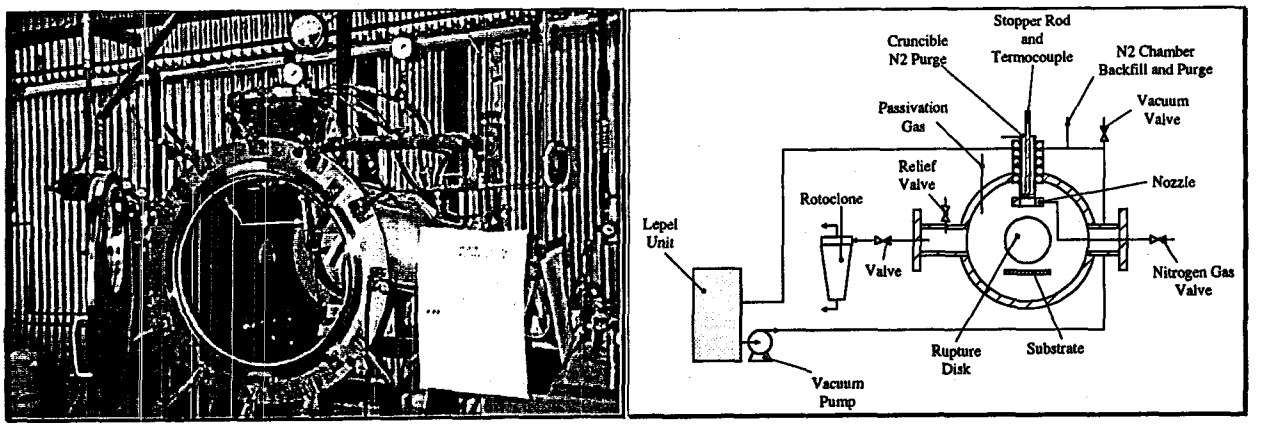

Figure 3. Picture and Sketch of the Spray Forming Unit at Alcoa Technical Center

5. Experimental Design

The initial approach taken for the design of the experiment was to test the hypothesis that the liquid fraction of the metal spray arriving at the deposit is controlling the level of bulk porosity. A series of calculations was made using the Spray model to determine the process conditions which will yield a given average solid fraction in the droplets at impact. The independent parameters were the atomizing gas pressure and flight distance. The dependent parameters were solid fraction, the droplet velocity, and average droplet size. Figure 4 is a plot showing the effects of the independent parameters on the predicted solid fraction. Since the dependent parameter of droplet velocity is most strongly correlated with pressure, a separate scale for this parameters is plotted along side the pressure scale.

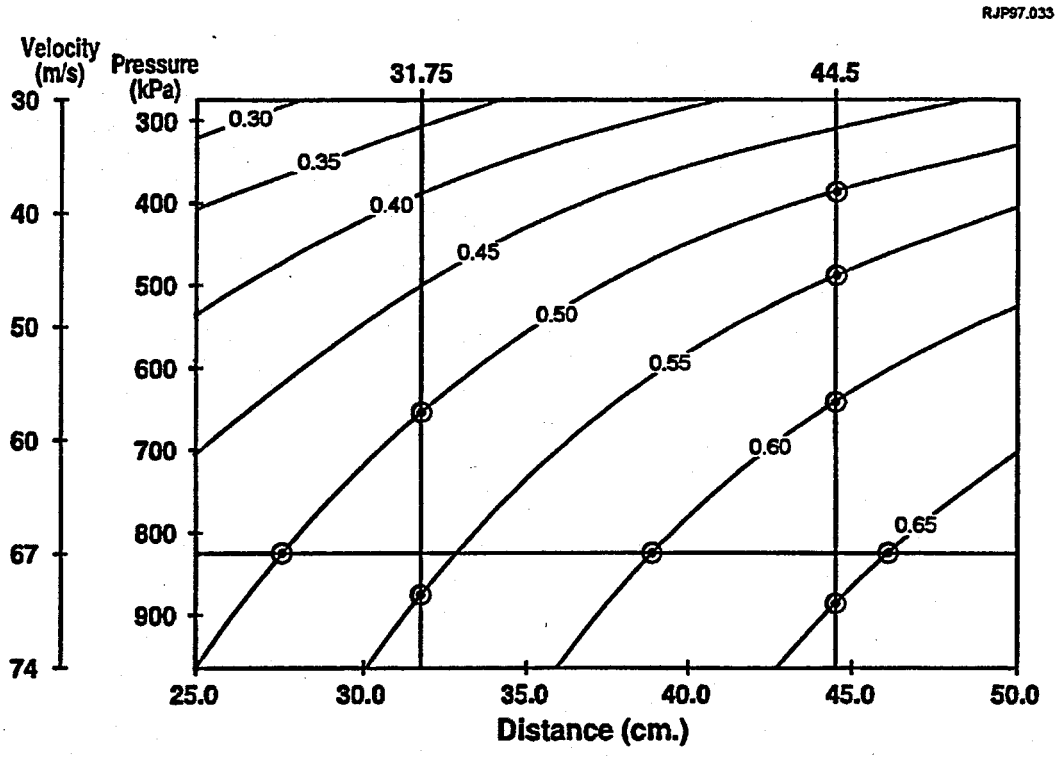

Figure 4. Predicted Fraction Solid From Spray Model

A test matrix was set up to examine the effects of spraying at four levels of liquid fraction obtained by using several levels of the atomizing gas pressure and flight distances. By using the model, it was possible to select test conditions in which the dependent parameter, solid fraction could be held constant while the independent parameters were varied at several levels. The experimental matrix of condition is noted on Figure 4. This experimental arrangement allowed us to test the effects of pressure, (velocity and droplet size) independent of the solid fraction of the droplets on porosity in the deposits.

Table 1. Sample Identification and Process Condition Test Matrix

Sample Number	Predicted Solid Fraction	Spray Distance (cm)	Spray Temp (°C)	Spray Pressure (kPa)
755019	0.540	37.5	766	793
755020	0.560	36.2	771	724
755021	0.538	29.2	771	800
755022	0.636	45.7	768	793
755023	0.600	44.5	771	414
755024	0.568	44.5	771	583
755397	0.610	44.5	771	690
755399	0.507	31.75	766	724
755400	0.550	31.75	766	896
755401	0.656	44.5	771	876

6. Results and Discussion

6.1 Spray Runs

Figure 5 is a photograph of cross-sections of deposits produced from the test matrix. Note the differences in shape and thickness. Comparing the shapes to the process conditions in Table 1, it is apparent that there is a correlation between the size of the deposit (sticking efficiency) and the predicted liquid fraction of the spray. For instance the very thin deposit of 755023 is believed to be due to a very low sticking efficiency resulting from the high solid fraction in the spray, whereas the exaggerated shapes of 755021 and 755400 are due to very "wet" spray conditions.

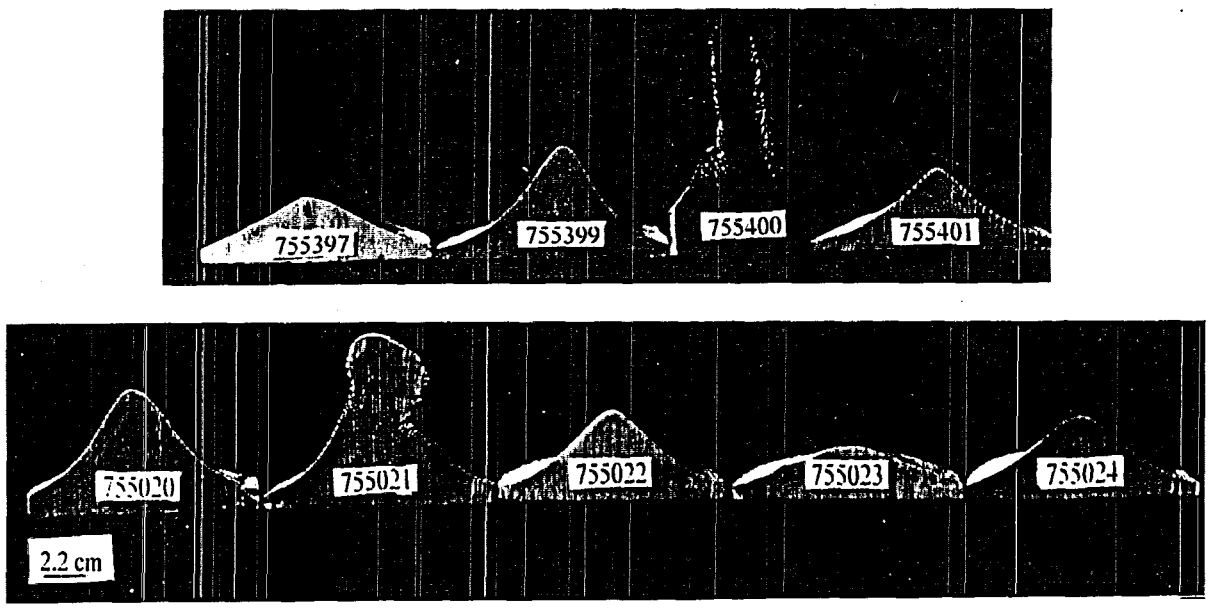

Figure 5. Photographs of Spray Formed Deposits

6.2 Porosity Measurements

The spray deposits shown in Figure 5 were sectioned along the centerline of the deposit and analyzed for porosity through the thickness. In general, two types of porosity were observed. One type of porosity is more or less spherical in shape ranging in size between 20 to 150 microns (Figure 6). This type of porosity is normally observed in the deposit sprayed with high fraction liquid (wet spray). It is believed that this type of porosity forms as a result of gas entrapment. The other type of porosity is more irregular shape with a size less than 10 microns (Figure 7). It is normally observed in the deposit sprayed with a low fraction liquid (dry spray) and forms when the solidification rate of the deposit exceeds the rate of deposition.

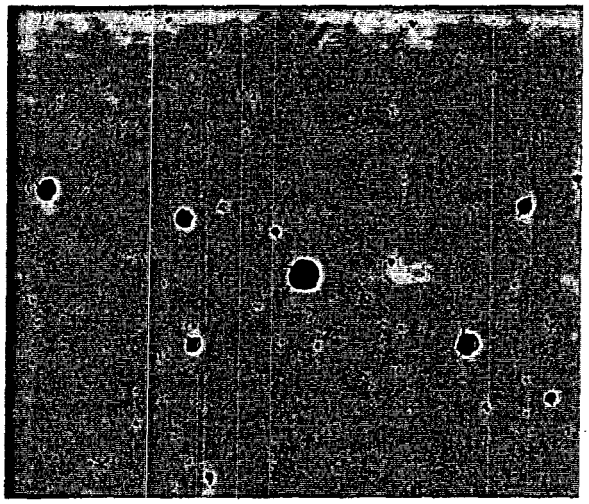

Figure 6. Typical "Wet Spray" Porosity

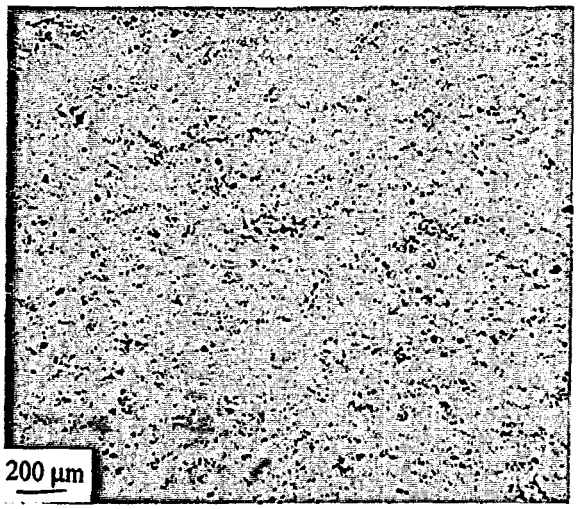

Figure 7. Typical "Dry Spray" Porosity

Under certain spray conditions, porosity can change from one type to another in the same deposit. For instance, as the thickness of a deposit grows during deposition, the spray distance decreases resulting in a "wetter" deposit from a hotter spray (due to less in-flight cooling of droplets) and a smaller chill effect from the substrate. The resulting porosity changes can be easily recognized from the change of the size and number of pores. Porosity from "wet" spray tends to be large in size but much fewer in number when compared to porosity from a "dry" spray. While it is an incomplete characterization of porosity, the count of the number of pores in a fixed volume offers a convenient measure to illustrate the change in porosity through the thickness of a deposit. In order to quantify the intensity of the porosity at the different locations through the thickness of a deposit, samples taken from the different locations through the thickness were polished and pictured at a 50X magnification using an optical microscope. The number of pores in each optical micrograph covering an area of 4 mm^2 was then counted visually. The measured pore count through the thickness of the bulk deposit is listed in Table 2 along with the processing conditions and predicted solid fraction. Figure 8 shows the variation of the number of pores through the thickness of the deposit. Note the break in the curve which is indicative of the change from "dry" porosity to "wet" porosity. There appears to be a critical deposit thickness at which the transition occurs.

Table 2. Pore Count Through the Thickness of Deposits

Sample Number	Predicted Solid Fraction	Spray Distance (cm)	Spray Temp (C)	Spray Pressure (kPa)	Porosity - no. of pores per 4 mm^2							Critical deposit thickness	Deposit Thickness at Top Surface
					Sample position from bottom surface (cm)								
					1.27	2.54	3.81	5.08	6.35	7.62	8.89		
755019	0.590	37.5	766	793	300	192	108	36				3.0	5
755020	0.560	36.2	771	724	288	160	140	12				2.5	5
755021	0.538	29.2	771	800	240	48	24	20				2.5	5
755022	0.636	45.7	768	793	300	250							2.5
755023	0.600	44.5	771	414	290								1.3
755024	0.568	44.5	771	583	200	190							2.5
755397	0.610	44.5	771	690	400	350							2.5
755399	0.507	31.75	766	724	270	196	190	155				2.4	5
755400	0.550	31.75	766	896	250	120	100	60	36	48	20	2.5	8.9
755401	0.650	44.5	771	876	320	250							2.5

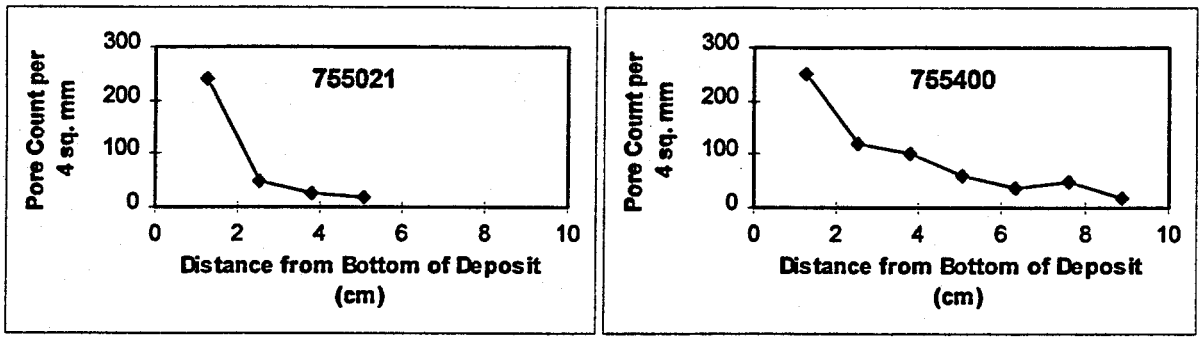

Figure 8. Through-Thickness Variation of Pore Count

6.3 Comparison with Deposition Model

In order to gain an understanding of the effects of solidification conditions on porosity formation the thermal histories of the deposits were analyzed using the transient deposition model. Further evidence for a critical deposit thickness was found. Figure 9 is a plot of the computed location of the top surface and solidus isotherm vs. spray time at a fraction solid of 0.6. This figure clearly shows that after a deposit reaches a threshold thickness, the mushy layer thickness grows rapidly as the spray continues. Some evidence for the growth of a mushy layer is seen in Figure 5 for deposits 755021 and 755400. In both of these deposits deformed top layers can be observed after the deposit reached a threshold thickness. The coarse outer surface suggests that semisolid layers were deformed under the pressure of the atomizing gas during spraying.

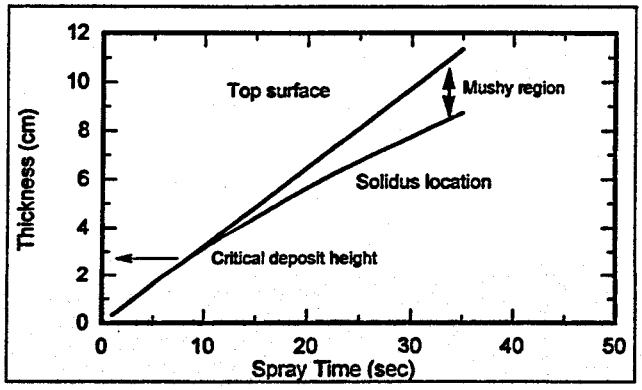

Figure 9. Location of the Top Surface and Solidus Isotherm vs. Spray Time (Solid Fraction = 0.6)

Figure 10 shows the computed effect of the solid fraction in the spray on the thickness of the deposit. Also plotted in Figure 10 is the measured location of the "dry" to "wet" transition point taken from the porosity measurements. A comparison of the two sets of data shows a consistent trend between the mushy threshold thickness and the transition from "dry" to "wet" spray conditions. Assuming the two are correlated, the offset between the two sets of data suggests that there may be an optimum thickness for the mushy zone. This is consistent with the arguments for a gas entrapment mechanism for large spherical pores [6,7] because trapped gas bubbles must solidify in a semi-liquid (mushy) layer to maintain their large spherical shape and size. Within a thin mushy zone, large bubbles cannot form within a thin mushy zone and smaller bubbles may migrate the short distance to the surface prior to solidification.

As the mushy zone grows thicker, larger gas bubbles can form and be trapped. In the present case, it is not possible to determine the thickness due to the poor spatial resolution of the porosity measurements (± 7 mm). Many estimated parameters were used in the Spray and Deposition models. Thus, there is potential for errors in the models because many of the input and boundary conditions are difficult to verify. Also, recall that for convenience, number of pores was used as a measure of porosity. The correlation relates only to the threshold in the number of pores. To optimize porosity, a similar correlation must also be established on the basis of the volume fraction and diameter of pores.

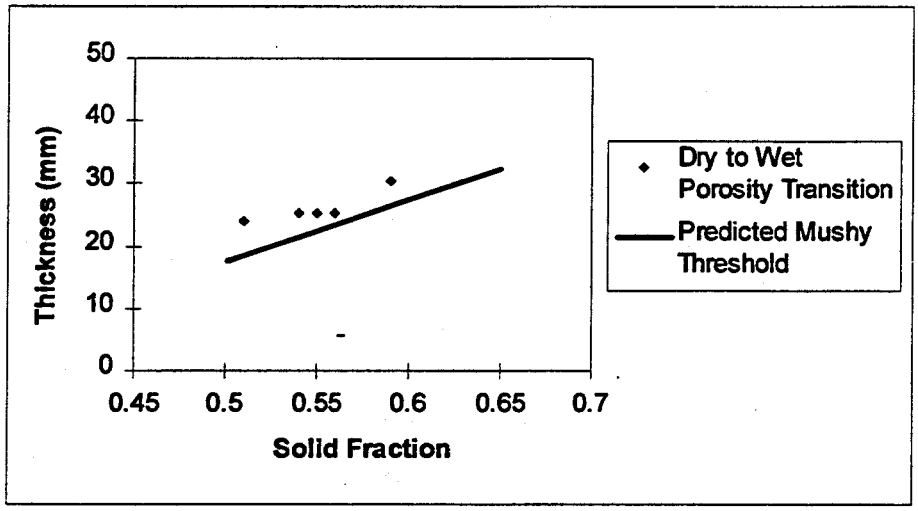

Figure 10. Predicted Mushy Threshold and Porosity Transition vs. Solid Fraction

7. Discussion

At the onset of this investigation, we set out to delineate the effects of the solid fraction of the spray on porosity in the bulk deposit. The data in Figure 10 and other published reports [8,9,10] support the strong influence of liquid fraction on porosity as shown in Figure 10. However, the implication from the transient deposition model of the existence of a threshold mushy zone thickness also suggests that solid fraction of the spray is affecting the porosity largely due to its effect on the thickness of the mushy layer. Surface temperature and porosity data of Grant and Cantor [8] also support this conclusion. Considering this mechanism, the key for optimizing "bulk" porosity in the deposit will be controlling the solid fraction in the spray according to the growth of a mushy layer thickness. An optimum porosity level will not necessarily occur at a fixed level of solid fraction in the spray under this scenario for different sets of processing conditions. It will be influenced by other thermal conditions which affect the solidification conditions in the deposit and the thickness of the mushy layer. To successfully implement such an approach, accurate models will be required to predict both the physical characteristics of the deposit as well as the thermal history and solidification path for a given process path.

In the present study, the rudimentary feasibility of such a model based approach has been demonstrated. For industrial applications, a coupled spray and deposition model representative of the transient and steady operating conditions of a particular spray forming unit will be required. The model can be used to predict the mushy transition thickness as a function of the parameter settings. By combining the model output with experimental data, the optimum mushy layer thickness and fraction solid can be determined.

8. Conclusions

1. Working models of the spray and deposition processes were developed for the spray forming unit at Alcoa Technical Center.

2. The successful application of numerical process models to design an experiment in which a model was used to predict dependent process parameters was demonstrated.

3. Porosity measurements of deposits produced by static spray tests show a rapid transition from a large number of small pores (dry porosity) to a small number of large pores (wet porosity). The transition thickness correlates with the predicted solid fraction of the spray.

4. Model predictions indicate there is a critical thickness in the deposit after which a thick mushy layer rapidly develops. The thickness of the mushy transition correlates directly with the solid fraction in the spray.

5. The porosity transition and mushy threshold follow the same trends with respect to the solid fraction in the spray and appear to be correlated.

6. The apparent correlation of the porosity transition and mushy threshold suggests there is an optimum mushy layer thickness to minimize porosity.

7. A model assisted methodology is proposed to determine an optimum mushy layer thickness.

9. Acknowledgments

The authors would like to recognize Mr. Jeffrey Shaw for his contributions in performing the spray tests and making porosity measurements. Partial support for this work provided by the U. S. Department of Energy under Agreement # DE-FC07-94 ID 13238 through use of the spray forming unit is acknowledged.

References

1. H. Lubanska, "Correlation of Spray Ring Data for Gas Atomization of Liquid Metals," J. Metals, p. 45, 1970 February.

2. M. K. Chyu, H. Ding, S. J. Pien, and J. Luo, 1995, "Modeling of Droplet Flow, Temperature and Solidification in a Spray Forming Process," HTD-Vol. 317-2, Proceedings of ASME Heat Transfer Division, Vol. 2, pp. 371-380 (1995)

3. H. Ding, M. K. Chyu, and S. J. Pien, "Three-Dimensional Numerical Simulation of Gas Dynamics Effects on Spray Forming Process," Proceeding of 31st ASME National Heat Transfer Conference, Houston, TX, August 3-6, Vol.1, HTD-VOL. 323, pp. 95-102 (1996).

4. S. J. Pien, M. K. Chyu and H. Ding, "Modeling of the Multi-Phase Transport Phenomena and Solidification in a Spray Forming Process with a Linear Nozzle," Proceedings of the 3rd International Conference on Spray Forming, pp. 45-52, Cardiff, UK, 1996 September.

5. U. Fritching and K. Bauckhage, 1994, "Spray Modeling in Spray Forming," FED-Vol. 201/HTD-Vol. 297, pp. 49-54, ASME (1994).

6. M. G. Chu, "Spray Forming," The Encyclopedia of Advanced Materials, eds. D. Bloor, R. J. Brook, M. C. Flemings and S. Mahajan, Pergamon Press, 1994, pp. 2624-2628.

7. M. G. Chu and S. John Pien, "Spray Forming Using A Linear Nozzle: Microstructure Analysis and Deposit Thermal Modeling," Proceedings of the Julian Szekely Memorial Symposium on Materials Processing, edited by H. Y. Sohn et al, TMS, 1997, pp. 423-438.

8. P. S. Grant and B. Cantor, Proceeding of International Conference on Advanced Synthesis of Engineer Structural Materials, 1992 August 31-September 02, San Francisco, CA, USA (J. J. Moore, E. J. Lavernia and F. H. Froes, eds.), ASM International, Materials Park, OH, (1993).

9. R. P. Underhill, P. S. Grant and B. Cantor, Processing, Properties and Applications of Metallic and Ceramic Materials, V2, Engineering Materials Advisory Services Ltd., United Kingdom (1992).

10. R. H. Bricknell, Metall. Trans. A, **17A**, 593 (1986).